

# The Relation Between Polycrystal Deformation and Single-Crystal Deformation

U. F. KOCKS

A phenomenological description of crystallographic slip and pencil glide in single crystals is outlined, with emphasis on the behavior under prescribed strains. Theoretical relations are established between these single-crystal properties and the behavior of quasi-homogeneous, quasi-isotropic polycrystals deforming uniformly on a macroscopic scale, at subdiffusive temperatures. Experimental comparisons between single crystals and polycrystals are reviewed, considering flow stress, work hardening, temperature and strain rate effects, and various effects of grain size.

IT is a fortunate circumstance that one does not need to understand dislocation theory in order to be able to discuss the physical processes underlying the behavior of a material, say, in a rolling mill. In principle, it is possible to proceed instead in a series of steps: to explain the behavior under real deformation conditions in terms of the behavior under idealized test conditions; to explain the properties of a polycrystalline aggregate under ideal test conditions on the basis of a phenomenological knowledge of single-crystal deformation properties; to explain the mechanical behavior of single crystals on the basis of dislocation theory; and so on down to the atomic or subatomic scale. The success of each step in the complete explanation often does not depend on the degree of our understanding of the other steps. However, the usefulness of these separations depends on the degree to which the intermediate steps in the model can be physically realized by intermediate experiments. For example, the behavior of a material under idealized test conditions is meaningful only to the extent to which friction and grip effects can be separated out.

The model used to describe the mechanical behavior of polycrystals in terms of that of single crystals is based on an idealized concept of a "polycrystal" and on an idealized concept of "single crystal properties."

A "polycrystal" is a polycrystalline specimen in which each cross section contains a large number of grains of each crystallographic orientation, distributed at random, and very few surface grains. Experimentally, it is virtually impossible to obtain specimens of any material without a preferred orientation. While it would be possible to analyze such textured specimens on the basis of the concepts to be outlined below, the theory would be more complicated and would be different for each case.

The influence of surface grains, on the other hand, would be well nigh impossible to consider theoretically. Experiments in which the number of surface grains is a small fraction of the total number of grains are possible but expensive. It is frequently overlooked that a wire containing 100 grains on the cross section has about one-third of its grains at the free surface. If one

wants the fraction of surface grains to be smaller than 10 pct, *the specimen diameter has to be at least 30 to 40 times the grain diameter*. Since it is often hard to obtain well-annealed specimens with grain sizes of less than 0.1 mm, the minimum wire size should thus be about 3 mm or  $\frac{1}{8}$  in. If one wishes to study grain size dependence up to a grain diameter of, say, 1 mm, one needs specimens of over 1 in. diam, and a suitably strong testing machine.

The models discussed in this paper also presuppose an idealized behavior of single crystals. For example, slip is assumed to be crystallographic but homogeneous. Since even this first-order description of single-crystal plasticity leads to strong interactions between neighboring grains, the physical realities of finite slip plane spacing and finite dislocation mean free path only lead to minor perturbations on the theory, which will be discussed in the last section of this paper. It is also ignored that there is generally some dislocation activity, or "micro-slip," on slip systems other than those providing the bulk of the macroscopic deformation.<sup>1,1a</sup> Finally, it is assumed that a unique work-hardening curve can be defined for a crystal of a given orientation under a given stress state, whereas in reality the reproducibility of stress strain curves is rarely better than  $\pm 5$  pct.

For all these reasons and more, one will probably have to be satisfied with an "explanation" of the mechanical behavior of polycrystalline specimens that establishes qualitative features and trends for *all* properties on the basis of *one* model, but in which an agreement of  $\pm 10$  pct between theory and experiment on any *specific* property must be regarded as very good. An explanation in this sense has, I believe, been established with respect to flow stress and work hardening, and their dependence on temperature, strain rate, and grain size, for materials of face-centered and body-centered cubic lattice structures, deforming homogeneously. On the other hand, deformation by the spreading of a Lüders band, the formation of deformation textures, and the processes limiting the ductility of polycrystalline specimens are not as yet understood to such a degree.

## THE YIELD LOCUS OF A SINGLE CRYSTAL

Grains in a polycrystal are generally not under such simple boundary conditions of stress and strain as single crystals in a tension test. One thus needs more

U. F. KOCKS is with the Materials Science Division, Argonne National Laboratory, Argonne, Ill., 60439.

This manuscript is based on an invited talk presented at the symposium on Deformation and Strength of Polycrystals, sponsored by the IMD Physical Metallurgy Committee, Detroit, Mich., October 14-15, 1968.

general criteria for the meaning of "yield" and "work hardening" in a grain than are used in free single crystals.

### The Schmid Law

For yield, the Schmid Law<sup>2</sup> may be stated in a form that is applicable to any stress state: *A single crystal yields on any particular slip system if the shear stress resolved on that slip plane and slip direction reaches a critical value, the "yield strength" on that slip system.* If the stress state is specified by the tensor  $\sigma_{ij}$ , and the yield strength on system  $s$  as  $\tau^s$ , this law may be expressed as

$$m_{ij}^s \sigma_{ij} \leq \tau^s \quad (i, j = 1, 2, 3) \quad [1]^*$$

\*Summation over repeated subscripts and superscripts is always implied unless the index is in parenthesis. The indices  $i, j, k, l, m, n$  run through 1, 2, 3; Greek indices run from 1 through 6; the superscript  $s$  runs through all slip systems, positive and negative.

where  $m_{ij}^s$  is the tensor transformation matrix to be defined below in more detail. The left-hand side of Eq. [1] is the properly resolved applied stress, while the right-hand side is a material property\* depending,

\* $\tau$  is a scalar while  $\sigma$  is a tensor; that is why the word "yield strength" is to be preferred over "yield stress." (See also McClintock and Argon,<sup>3</sup> p. 279.)

for example, on the defect structure or, indirectly, on the previous strain history. The equality sign in Eq. [1] has to hold for every system that is active at a particular time; the inequality (or the equality) may hold for other systems. It is impossible to apply stresses so high that they would violate Eq. [1];  $\tau^s$  for each overloaded system would then have risen along with the applied stress through work hardening.

The magnitude of the yield strength,  $\tau^s$ , may, in some cases (for example, when it is controlled by the Peierls stress), depend on other components of the applied stress, such as the hydrostatic pressure or the normal stress on the slip plane (which affect the dislocation core structure). Such cases, in which the Schmid Law<sup>1</sup> is said to be violated, shall be excluded from treatment in this paper, although most of our conclusions will be based on *strain* arguments and would thus apply even for these materials.

For the case of single slip in system  $s = 1$  in a single crystal under pure tension in the  $z$  direction,  $m_{ij}^s$  degenerates into the Schmid factor

$$m \equiv m_{zz}^1 = \cos \phi \cdot \cos \lambda \quad [2a]$$

where  $\phi$  and  $\lambda$  are the angles between the slip plane normal and the slip direction on the one hand and the tensile axis on the other. If one defines  $\mathbf{n}_1^s$  as the slip plane normal of system  $s$ ,  $\mathbf{n}_2^s$  as the slip direction of system  $s$ , and  $(\mathbf{a}_1, \mathbf{a}_2, \mathbf{a}_3)$  as the three unit vectors defining the coordinate system in which the applied stress tensor is given, then Eq. [2a] may be generalized to

$$m_{ij}^s = \mathbf{n}_1^{(s)} \cdot \mathbf{a}_i \quad \mathbf{n}_2^{(s)} \cdot \mathbf{a}_j \quad [2b]$$

It is often convenient to write out the two scalar products in [2b] in terms of the components of all the unit vectors in some third, "neutral" coordinate system such as the cube edge directions in materials with cubic lattice symmetry. Characterizing this third coordinate system with the dummy indices  $k$  and  $l$ , we have

$$m_{ij}^s = n_{1k}^{(s)} a_{ik} n_{2l}^{(s)} a_{jl} \quad (k, l = 1, 2, 3) \quad [2]$$

as the most general definition of the tensor transformation matrix.

If one wants to retain the possibility of having different yield strengths in the forward and backward direction on the same slip plane (for applications to work hardened materials, to twinning, and to slip in a direction not perpendicular to a mirror plane, as it occurs in bcc crystals), one should label each conventional "slip system" with two different numbers  $s$ , one for the positive and one for the negative direction. In this paper we shall use the term "slip system" in this directional sense.  $\tau^s$  is then positive by definition, as is the increment of shear in each system:

$$d\gamma^s \equiv 2 \cdot |d\epsilon_{12}^s| \quad [3]$$

The total strain  $d\epsilon_{ij}$  in a crystal in which the equality in Eq. [1] is fulfilled in any number  $S$  of systems  $s$  is (using  $\sigma_{ij} = \sigma_{ji}$ )

$$d\epsilon_{ij} = \frac{1}{2} (m_{ij}^s + m_{ji}^s) d\gamma^s \quad (s = 1, \dots, S) \quad [4]$$

Inasmuch as the strength-strain relations during plastic deformation depend very sensitively on the strain path, through the path dependence of the development of the dislocation structure with strain, it is appropriate to use differential strains rather than finite strains which are based on an arbitrary initial state.\*

\*For shape measurements on single crystals, it is appropriate to use finite deformation gradient matrices.<sup>4</sup>

Eq. [1] is merely a special form of the general yield criterion

$$f(\sigma_{ij}) \leq c \quad [5]$$

commonly used in the mathematical theory of plasticity. Similarly, Eq. [4] would follow from Eq. [1] by use of the "associated flow rule"

$$d\epsilon_{ij} = \frac{\partial f}{\partial \sigma_{ij}} \cdot d\sigma \quad [6]$$

which is another basic hypothesis of this theory. Eq. [6] is equivalent<sup>5</sup> to the statement that the function  $f$  in the yield criterion [5] is also the plastic potential.\*

\*For a good discussion of the application of the concepts of the mathematical theory of plasticity to physical problems, see McClintock and Argon.<sup>3</sup>

If one inverts  $m$  in the equality [1] and then multiplies  $\sigma_{ij} (= \sigma_{ji})$  with  $d\epsilon_{ij}$  as expressed in Eq. [4], one can see that the work done by the external forces equals the work done in the slip systems:

$$\sigma_{ij} d\epsilon_{ij} = \tau^s d\gamma^s \quad [7]$$

### The Yield Locus

The above concepts may be expressed by means of a geometrical representation called the yield surface or yield locus. For this purpose it is useful to define single row (or column) matrices for the six independent components of stress and strain and for certain combinations of direction cosines, as follows:

$$\{\sigma_\nu\} \equiv \{\sigma_{11}, \sigma_{22}, \sigma_{33}, \sigma_{23}, \sigma_{31}, \sigma_{12}\} \quad [8a]$$

$$\{\epsilon_\nu\} \equiv \{d\epsilon_{11}, d\epsilon_{22}, d\epsilon_{33}, 2d\epsilon_{23}, 2d\epsilon_{31}, 2d\epsilon_{12}\} \quad [8b]$$

$$\{m_\nu\} \equiv \{m_{11}^s, m_{22}^s, m_{33}^s, m_{23}^s + m_{32}^s, m_{31}^s + m_{13}^s,$$

$$m_{12}^s + m_{21}^s \} \quad [8c]$$

so that Eqs. [1] and [4] may be rewritten as follows:

$$m_{\nu}^s \sigma_{\nu} = \tau^s \quad \text{for each active system} \quad [1a]$$

( $\nu = 1, \dots, 6$ )

$$m_{\nu}^s \sigma_{\nu} \leq \tau^s \quad \text{for each inactive system} \quad [1b]$$

and

$$d\epsilon_{\nu} = m_{\nu}^s d\gamma^s \quad (s = 1, \dots, S) \quad [4a]$$

One may further complement these equations by defining the increments of lattice rotation

$$d\omega_k = r_k^s d\gamma^s \quad [9]$$

with

$$\{d\omega_k\} \equiv \{2d\omega_{23}, 2d\omega_{31}, 2d\omega_{12}\} \quad [10a]$$

and

$$\{r_k^s\} \equiv \{m_{23}^s - m_{32}^s, m_{31}^s - m_{13}^s, m_{12}^s - m_{21}^s\} \quad [10b]$$

Eqs. [1a] may be interpreted as describing a set of planes (one for each system) in a six-dimensional space whose coordinates are the six components of stress [8a]. The  $m_{\nu}^s$  are the inverse intercepts on the  $\nu$  axis of the  $s$  plane. Similarly, Eq. [4a] shows that the direction of the strain increment due to a single slip system  $s$  is in the direction of  $m_{\nu}^s$ , *i.e.* the normal to the plane  $s$ . (The coordinate system used in the six-dimensional space is assumed to be orthogonal.) Thus, the strain increment is perpendicular to the yield locus as suggested by Eq. [6].

To illustrate the usefulness of these concepts, let us derive the yield locus of an hexagonal single crystal yielding in basal slip only.<sup>6</sup> Here, the yield stress is infinite in all directions of the six-dimensional stress space except in the two-dimensional plane representing shears in the basal plane. There are six slip directions in the basal plane (three positive and three negative), and thus there are six facets of the yield surface, which intersect the two-dimensional plane in question in straight lines. The yield locus, by virtue of the inequality in Eq. [1] or [1b], is the inner envelope of these lines. Fig. 1 shows the requisite picture.

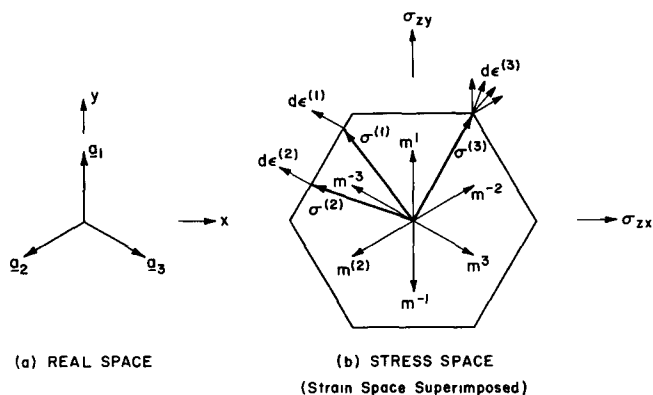


Fig. 1—(a) Definition of a coordinate system in the basal plane (perpendicular to  $z$ ) of an hexagonal crystal. The slip vector  $n_2^s$  may be in the directions  $a_1, -a_1, a_2, -a_2, a_3, -a_3$ . (b) Section at  $\sigma_{xx} = \sigma_{yy} = \sigma_{zz} = \sigma_{xy} = 0$  through the yield locus of an hexagonal crystal yielding in basal slip. The stress states  $\sigma^{(1)}$  and  $\sigma^{(2)}$  will lead to the strain state  $d\epsilon^{(1)} = d\epsilon^{(2)}$ ; any one of the strain increments  $d\epsilon^{(3)}$  will demand the same stress  $\sigma^{(3)}$ .

Let us apply, in turn, three different stress states to the crystal represented by Fig. 1, and let all of the components of each of the stress states in turn be raised proportionally until the yield surface is reached. The three stress states at this stage are called  $\sigma^{(1)}$ ,  $\sigma^{(2)}$ , and  $\sigma^{(3)}$ , and are represented by arrows in Fig. 1(b). In the first and second case, any strain increment upon yielding will have to be in the "direction" specified by the arrows  $d\epsilon^{(1)}$  and  $d\epsilon^{(2)}$ ; they are the same, although the stress directions are different. The Schmid law says nothing about *how much* strain will occur upon yielding, only that it must be positive (or zero) in the direction specified.

The stress state  $\sigma^{(3)}$  was chosen in a special way, namely such that two systems be activated simultaneously as soon as the yield surface is reached. Again, the Schmid law does not specify how much strain will occur on either system, only that it must be positive (or zero) in the direction of the outward normal to each of the facets. Thus, the total strain increment may be in any direction contained within the fan of normals  $d\epsilon^{(3)}$  in this corner of the yield surface. This is a generalization of Eq. [6] for discontinuities in the yield surface, *i.e.*, when Eq. [5] degenerates into a set of simultaneous equations.

The case of basal slip in hexagonal crystals was deliberately chosen to be simple. In this case, the use of the yield locus does not significantly advance our understanding of the process. The usefulness of the method will be more evident if we treat one more example that has been extensively studied:<sup>6-8</sup> fcc crystals slipping on  $\{111\}$  planes in  $\langle 110 \rangle$  directions. Since there are twelve positive and twelve negative slip systems, one will obviously have to find a straightforward procedure to define the yield surface. Such a procedure is given by Eqs. [1a], [8c], and [2]. For a cubic crystal, it is sensible to choose as the coordinate system  $a_i$  in Eq. [2] the cubic axes and not a coordinate system defined by a specific external stress state. Then,\*  $a_{ik} = \delta_{ik}$  and  $a_{jl} = \delta_{jl}$ ; the terms  $n_{ik}^s$

\* $\delta_{ij} = 1$  for  $i = j$ ;  $\delta_{ij} = 0$  for  $i \neq j$ .

and  $n_{2j}^s$  become the normalized Miller indices of the slip plane normal and slip direction, respectively. The matrix  $m_{\nu}^s$  (Eq. [8c]) for all slip systems is then easily obtained. It is given in Table I, where we again assume

$$\tau^s = \tau \quad \text{for all slip systems } s \quad [11]$$

For completeness, Table I includes the rotation matrix  $r_k^s$  also.<sup>8</sup> Now each  $m_{\nu}^s$  defines the inverse intercept on the  $\nu$  axis of the facet belonging to slip system  $s$ . For a visualization of the yield surface, one only needs to select specific sections through the six-dimensional space by setting three stresses  $\sigma_{\nu} = 0$  and plotting the other three. Fig. 2 shows a section obtained in this way for  $\sigma_{22} = \sigma_{33} = \sigma_{23} = 0$ , with  $\sigma_{12}$  plotted in the X-direction, and so on.

Fig. 3 was obtained by the same method but by use of the coordinate system appropriate for one particular slip system. The figure was derived merely to show the comparison to basal slip in the hexagonal crystal. The yield surface is now no longer infinite in all directions other than those contained in the plane corresponding to basal slip. For example, plotting a tensile stress perpendicular to the slip plane

as the third direction, as in Fig. 3, shows that six systems will get simultaneously activated in fcc crystals, although in a much less efficient way.

### Corners of the Yield Locus

If one looks at the corners in Figs. 2 and 3, one finds that either four, six, or eight systems are simultaneously activated. Drawing other sections through the yield surface, one could have found<sup>6</sup> corners in which three or five systems are activated; further-

Table I. The Matrix  $m_p^s$  of All Single Slip Facets of the fcc Yield Locus, Referred to Cubic Axes, and the Miller Indices of the Plastic Rotation Axes,  $r_k^s$

Slip System ( $\pm s$ )			$m_p^s = \pm 1/\sqrt{6} \times$						$r_k^s$		
Names*	Plane	Dir.	11	22	33	23	31	12	23	31	12
			1	2	3	4	5	6	1	2	3
a	PK	1 1 $\bar{1}$ 0 1 1	0	1	$\bar{1}$	0	1	1	2	$\bar{1}$	1
b	PQ	1 0 1	1	0	$\bar{1}$	1	0	1	1	2	$\bar{1}$
c	PU	1 $\bar{1}$ 0	1	$\bar{1}$	0	1	$\bar{1}$	0	$\bar{1}$	$\bar{1}$	2
d	QU	1 $\bar{1}$ $\bar{1}$ 0 1 $\bar{1}$	0	$\bar{1}$	1	0	$\bar{1}$	1	2	1	1
e	QP	1 0 1	1	0	$\bar{1}$	$\bar{1}$	0	$\bar{1}$	$\bar{1}$	2	1
f	QK	1 1 0	1	$\bar{1}$	0	$\bar{1}$	$\bar{1}$	0	1	$\bar{1}$	2
g	KP	1 $\bar{1}$ 1 0 1 1	0	$\bar{1}$	1	0	1	1	2	$\bar{1}$	1
h	KU	1 0 $\bar{1}$	1	0	$\bar{1}$	1	0	$\bar{1}$	1	2	1
i	KQ	1 1 0	1	$\bar{1}$	0	1	1	0	$\bar{1}$	1	2
j	UQ	1 1 1 0 1 $\bar{1}$	0	1	$\bar{1}$	0	$\bar{1}$	1	2	1	1
k	UK	1 0 $\bar{1}$	1	0	$\bar{1}$	$\bar{1}$	0	1	$\bar{1}$	2	$\bar{1}$
l	UP	1 $\bar{1}$ 0	1	$\bar{1}$	0	$\bar{1}$	1	0	1	1	2

\*The single lower-case letter is for use in Table II, the pair of capital letters is the designation usually used by this author,<sup>6,9</sup> which is useful for the study of dislocation interactions

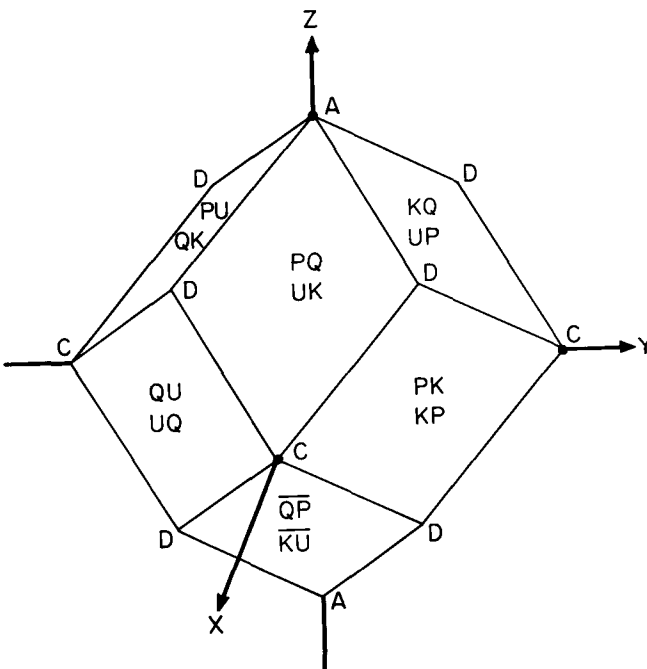


Fig. 2—Section through fcc yield surface for

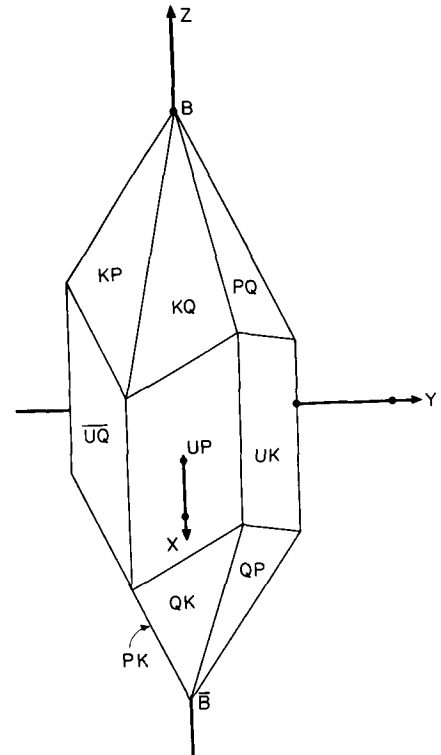
$$\sigma = \begin{bmatrix} Z & X & Y \\ X & 0 & 0 \\ Y & 0 & 0 \end{bmatrix}$$

in cubic coordinates.

Fig. 3—Section through fcc yield surface in coordinates of glide system, UP:

$$(x, y, z) = (111, 1\bar{1}0, 11\bar{2});$$

$$(\sigma_{xy}) = \begin{bmatrix} Z & X & Y \\ X & 0 & 0 \\ Y & 0 & 0 \end{bmatrix}$$



more, there are the edges in which only two systems are activated. In six dimensions, it takes six planes to make a real "corner", whose cone of normals has a finite angular extent in every one of the six dimensions. When fewer facets meet, the possible strain directions are restricted in some dimensions, and it is arbitrary whether one calls such places corners or edges.

Now it is evident that slip can never cause any volume changes and, conversely, that a hydrostatic stress can never have a resolved shear stress on any slip system (see Eqs. [1] and [2], remembering  $n_{1i}^{(s)} n_{2i}^{(s)} = 0$ ). Thus, all yield surfaces will always extend to infinity in the  $\{111000\}$  direction, and no corner can have a cone of normals extending into more than five dimensions. We shall call "corners of the yield locus" only such stress states as are capable of activating a finite range of strains in all remaining five dimensions and we shall call the process involved "polyslip".<sup>6,10</sup> All stress states that activate more than one system but do not qualify as corner states, are called "edge states" and the process involved is called "multiple slip".

If one were to prescribe an arbitrary direction of straining, this direction would in general be normal to the yield surface only at one of the corners. Thus, the stress state necessary to achieve such a deformation will have to be one of a number of discrete stress states. This is analogous to the case of a prescribed arbitrary stress, in which the response of the specimen will be any one of a number of discrete straining directions.

Most single crystal experiments are performed on wires, in which the proximity of free surfaces everywhere forces the stress direction to be in the wire axis (even though the amount of the stress may not be prescribed by a dead weight, but rather by the specimen's response to a prescribed extension rate). In

such tests, single crystals will generally yield in single slip. The strain state will by no means be a pure extension; for example, the cross section will generally change shape.

The case of a completely prescribed "direction" of straining, in all components, is impossible to realize in practice. Many technological forming operations, such as forging in a closed die, are, however, of this general type. Drawing a wire through a die<sup>11</sup> or compressing a specimen under lateral constraints ("plane strain compression")<sup>11a,b</sup> are relatively simple tests that may be performed even on single crystals and that approximate prescribed strain conditions. In all such cases, the stresses are not well known because of the unavoidable friction at the contact faces.

If the discrete stress states leading into any corner *c* of the yield surface are defined by  $\sigma_\nu^c$ , and if Eq. [11] holds, it is sensible to define a normalized corner arrow  $M_\nu^c$  such that, by virtue of the yield criterion, Eqs. [1a] and [1b],

$$M_\nu^c m_\nu^s = 1 \quad \text{for all (s) in (c)} \quad [12a]$$

$$(\nu = 1, \dots, 6)$$

$$M_\nu^c m_\nu^s < 1 \quad \text{for all (s) not in (c)} \quad [12b]$$

Eq. [12a] defines *M* only in its deviatoric (*i.e.*, nonhydrostatic) components,\* as indeed the stress to

\*The deviatoric components  $A_{ij}^d$  of a tensor *A* are defined as  $A_{ij}^d = A_{ij} - A_{kk}\delta_{ij}$ . activate a certain slip system combination can only be defined in its deviatoric components. They are

$$\sigma_\nu^c = M_\nu^c \tau \quad \text{for each corner} \quad [13]$$

In practical cases, it is usually not the hydrostatic stress that is zero, but one or two of the individual normal stress components. One may thus dispose of the arbitrary hydrostatic component of the corner arrows *M* in the same way and make as many of the components for  $\nu = 1, 2, 3$  zero as possible. In this definition, the  $M_\nu^c$  matrix for fcc crystals is given in Table II.<sup>6</sup> In contradistinction to the  $m_\nu^s$  matrix,  $M_\nu^c$  has to be found by trial and error (or by a systematic search).

Eq. [13] is the analogue of Eq. [1a], for the case of prescribed strains. Similarly, an analogue of Eq. [4a] describes the relation between strains and shears. It is most easily derived<sup>12</sup> by writing down the work expression

$$\sigma_\nu^c d\epsilon_\nu = \tau M_\nu^c d\epsilon_\nu \quad (\nu = 1, \dots, 6) \quad [14]$$

and equating it with the work done in the active slip systems,  $\tau^s d\gamma^s$ . If work hardening is isotropic (Eq. [11]), and if the strain increment is, as usual, prescribed only in its deviatoric components  $d\epsilon_k^d$ , it follows that

$$M_\nu^c d\epsilon_\nu^d = \sum_s d\gamma^s \equiv d\Gamma \quad [15]$$

where  $\Gamma$  is the algebraic sum of shears defined by this equation.

Just as  $m_\nu^s$  degenerates into the Schmid factor\*

\*The symbol *m* is variously used for the quantity defined in Eq. [16] or its inverse.

$$m = \frac{\tau}{\sigma} = \frac{d\epsilon_\sigma}{d\gamma} \quad \text{for uniaxial stress,} \quad [16]$$

so  $M_\nu^c$  degenerates into the Taylor factor

$$M = \frac{d\Gamma}{d\epsilon} = \frac{\sigma_\epsilon}{\tau} \quad \text{for uniaxial strain.} \quad [17]$$

Here  $d\epsilon_\sigma$  means the component of the strain in the direction of the applied stress, and  $\sigma_\epsilon$  the component of the stress in the direction of the applied strain, see Fig. 4. These equations follow from Eqs. [1a] and [4a], and from Eqs. [13] and [15], respectively.

Values for *M* in tension (or compression) in various orientations in the stereographic unit triangle have been obtained by Taylor.<sup>13</sup> Fig. 5 reproduces contours obtained by computer.<sup>14</sup> There are five regions of the triangle in which the final corner of the yield surface is the same.

From the point of view of the crystallographic relation between the various slip systems activated by a given corner stress state, and the ensuing dislocation interaction possibilities, corner states fall into five different "polyslip types".<sup>12</sup> These are listed in Fig. 6 for fcc crystals. Each type is represented in one of the five regions of the unit triangle for prescribed uniaxial strain. The various polyslip types may be activated in a free single crystal by special stress states,

Table II. The Matrix  $M_\nu^c$  of All Polyslip Corner Stress States in the fcc Yield Locus, Referred to Cubic Axes, and the Miller Indices  $R_k^c$  of Strain-Free Plastic Rotation Axes

Corner(±c)	Bishop <sup>7</sup> Name*	$M_\nu^c = \pm\sqrt{6} \times$						$R_k^c$			$M_\nu^c m_\nu^s = 1$ for these slip systems
		11	22	33	23	31	12	23	31	12	
		1	2	3	4	5	6	1	2	3	
2	A 1	1	0	0	0	0	0	Any			bcefhikl acd̄fḡijl abdegh̄ijk
3	2	0	1	0	0	0	0				
1	3	0	0	1	0	0	0				
28	B 1	0	0	0	+1/2	+1/2	+1/2	+1	+1	+1	abēf̄gi
27	2	0	0	0	-1/2	+1/2	+1/2	-1	+1	+1	ac̄gh̄kl
26	3	0	0	0	+1/2	-1/2	+1/2	+1	-1	+1	bcdējl
25	4	0	0	0	+1/2	+1/2	-1/2	+1	+1	-1	d̄fh̄ijk
4	C 1	0	0	0	1	0	0	Any			bcēf̄h̄ikl̄ acd̄f̄ḡijl abdegh̄ijk
5	2	0	0	0	0	1	0				
6	3	0	0	0	0	0	1				
17	D 1	1/2	0	0	0	+1/2	+1/2	0	1	1	abḡikl acef̄gh deh̄ijl
20	2	1/2	0	0	0	-1/2	-1/2				
19	3	1/2	0	0	0	+1/2	-1/2				
18	4	1/2	0	0	0	-1/2	+1/2				
13	5	0	1/2	0	+1/2	0	+1/2	1	0	1	abēf̄j̄l bc̄dēgi ac̄h̄ij̄k d̄f̄gh̄kl̄
16	6	0	1/2	0	-1/2	0	-1/2				
14	7	0	1/2	0	-1/2	0	+1/2				
15	8	0	1/2	0	+1/2	0	-1/2				
21	9	0	0	1/2	+1/2	+1/2	0	1	1	0	ēf̄ḡij̄k̄ abdf̄h̄i ac̄dēkl̄ bc̄gh̄j̄l
24	10	0	0	1/2	-1/2	-1/2	0				
23	11	0	0	1/2	+1/2	-1/2	0				
22	12	0	0	1/2	-1/2	+1/2	0				
9	E 1	0	+1/2	-1/2	+1/2	0	0	Any			abdf̄gh̄j̄l ac̄dēḡijk bc̄ef̄gh̄ik̄ abdēh̄ik̄l̄ bcdf̄ḡikl acefh̄ijl
10	2	0	+1/2	-1/2	-1/2	0	0				
7	3	-1/2	0	+1/2	0	+1/2	0				
8	4	-1/2	0	+1/2	0	-1/2	0				
11	5	+1/2	-1/2	0	0	0	+1/2				
12	6	+1/2	-1/2	0	0	0	-1/2				

Note: A constant  $p^c$  was added to each  $M_\nu^c$ ,  $M_\nu^s$ , and  $M_\nu^s$  such as to make zeroes out of as many of them as possible.

\*A, B, C, D, E are the crystallographically distinct types of polyslip investigated by Kocks.<sup>6,12</sup>

such as  $\langle 100 \rangle$  tension,  $\langle 111 \rangle$  tension,  $\{100\}\langle 010 \rangle$  shear, and so forth.<sup>12</sup> In this manner the respective work hardening curves have been obtained by Kocks.<sup>12</sup> Hosford<sup>15</sup> has later determined the same polyslip curves in "plane strain compression".

### Rotations

The number of systems activated in any corner or edge state may be larger than the number of dimensions in which the cone of normals has a finite extent. In this case, one says that they do not form a set of independent slip systems. This term is somewhat misleading,<sup>16</sup> because dislocation motions in, for example, eight different slip systems may be entirely uncoupled from each other. However, different combinations of slip may give the same macroscopic strain in all directions; they would give different rotations of the crystal lattice with respect to the specimen surfaces. Such "plastic rotations" can, on the other hand, not be enforced by any boundary conditions on the specimen. It is in this sense that resolution of an applied stress or strain state into more than five slip systems cannot be unique, and that such a set of slip systems may be called interdependent.

When eight slip systems meet in a corner, there are three degrees of freedom left, and thus all rotations are possible. When there are only six slip systems, however, rotations must be restricted to a single axis. To find this axis, it is best to try to produce a *pure* rotation by maximizing the *differences* between various slip systems of the combination. Maximum difference between the contributions of *coplanar* slip systems show, in the case of  $\langle 111 \rangle$  tension of fcc crystals, that the arbitrary rotation can only be a twist around the tensile axis. Table II lists the Miller indices of the axis around which arbitrary additional rotations are allowed, under  $R_k^c$ .

### Card Glide and Pencil Glide

Ice slips on a crystallographic slip plane, but the slip direction is approximately the direction of maximum resolved stress in this plane. This situation is easily described in stress space. The yield locus is a circle in the plane containing all shears on the slip plane, and it is infinite in all four perpendicular direc-

tions. The direction of the stress state and the direction of the strain state are thus parallel in this plane (Eq. [6]), although there may be additional stress components out of this plane. This behavior may be described as "card glide".

"Pencil glide" is very similar: here the slip *direction* is crystallographically prescribed, but the slip *plane* is that of maximum resolved shear stress containing the crystallographic slip direction. Since the terms slip plane and slip direction are interchangeable from a point of view of macroscopic strain, any yield locus for pencil glide in a particular slip direction can also be described by a circular cylinder. For example, if there were an hexagonal crystal that deformed in pencil glide on any prismatic plane in the direction normal to the basal plane, its yield locus would be identical to that of ice described above.

In algebraic form, the yield condition for card glide or pencil glide, with a crystallographically prescribed slip plane or slip direction in the x-coordinate, is<sup>17</sup>

$$\sigma_{xy}^2 + \sigma_{xz}^2 = \tau^2 \quad [18]$$

Pencil glide is often a good description of what happens in bcc single crystals: the slip direction is

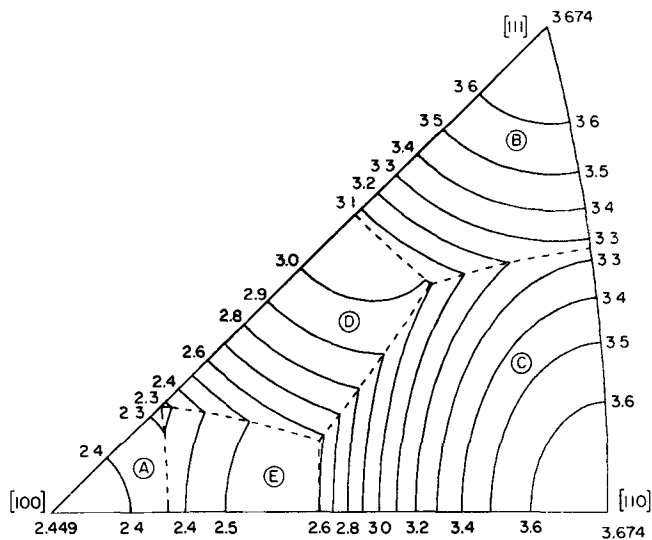
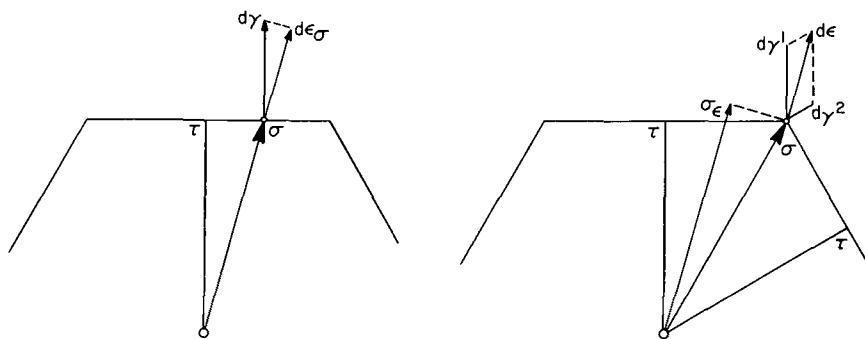


Fig. 5—The Taylor factor  $M$  for tension in fcc crystals, as a function of the orientation of the tensile axis. According to Chin *et al.*<sup>14</sup>



a) PRESCRIBED STRESS CASE:

SCHMID FACTOR

$$m = \frac{\tau}{\sigma} = \frac{d\epsilon_{\sigma}}{d\gamma}$$

b) PRESCRIBED STRAIN CASE:

TAYLOR FACTOR

$$M = \frac{d\gamma^1 + d\gamma^2}{d\epsilon} = \frac{\sigma_{\epsilon}}{\tau}$$

Fig. 4—Relations between external variables  $\sigma$ ,  $d\epsilon$  and slip system variables  $\tau$ ,  $d\gamma^i$ .

of  $\langle 111 \rangle$  type and the slip plane is, on the average, noncrystallographic. In other cases,  $\{110\}$  is a crystallographically preferred slip plane. If again one treats the terms slip plane and slip direction as interchangeable, the latter case is exactly equivalent to slip in fcc crystals, and thus the yield surfaces are identical.

The yield locus for pencil glide may then be obtained from the fcc yield locus by eliminating any distinction between the slip directions in the fcc  $\{111\}$  plane. This amounts to replacing a number of hexagonal cylinders by circular cylinders. However, not all corners and edges are taken out of the yield surface, because the different cylinders belonging to different fcc slip planes (bcc slip directions) intersect to form some edges and corners. Figs. 7 and 8 show the bcc pencil glide equivalents to Figs. 2 and 3. It is worth noting that there are some "points" where two cylinders intersect, which are, however, not corners in any sense of the word: they have a unique normal.

Those points on Figs. 7 and 8 that look like true corners are, however, not "corners" by the definition used here either: their cones of normals extend into only three or four dimensions, not into five. Thus,

there are no polyslip corners at all in the bcc pencil glide yield surface, and by far the majority of all prescribed strain states would be satisfied by a combination of fewer slip systems. Also, there is never any ambiguity of slip system selection that could lead to arbitrary superimposed rotations.<sup>18</sup>

The four slip directions available in bcc crystals are thus ample to insure the possibility of plastic relief of any (deviatoric) prescribed strain, *i.e.*, to insure that the yield surface is closed in five dimensions. Would three slip directions have been enough, in general? It is easy to see that three slip directions aligned with the edges of a cube could not produce any length change in any of the edge directions, no matter what slip plane were used.

The general condition for pencil glide to provide a complete set of independent modes is that three slip directions be available which are not coplanar and which do not include any right angle.

### Work Hardening and Latent Hardening

Work hardening in single crystals is usually described by a series of yield strength vs shear curves

Fig. 6—The five types of polyslip.

A	B	C	D	E
[100] Tension	[111] Tension	{100}[010] Shear	[100] Compression +{100}[011] Shear	{100}[010] Shear +{110}[110] Shear
1 0 0 0 0 0 0 0 0	0 1 1 1 0 1 1 1 0	0 1 0 1 0 0 0 0 0	1 1 1 1 0 0 1 0 0	1 1 0 1 1 0 0 0 0

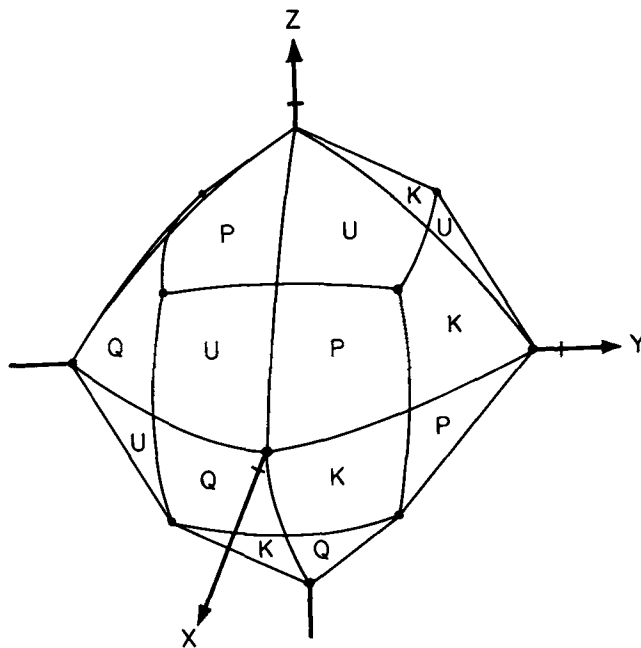
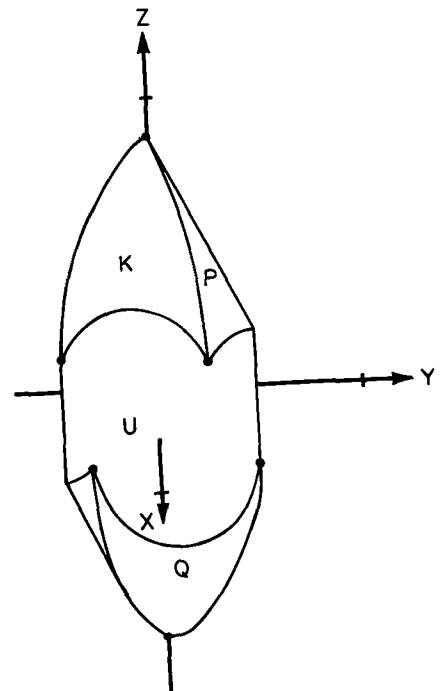


Fig. 7—Section through the yield surface for bcc pencil glide, in cubic coordinates.

$$\sigma = \begin{bmatrix} Z & X & Y \\ X & 0 & 0 \\ Y & 0 & 0 \end{bmatrix}.$$

Fig. 8—Section through bcc yield surface. X and Y: shear stresses in glide direction; Z: normal stress in glide direction. Qualitative.



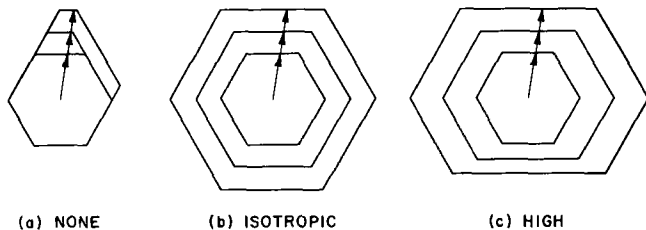


Fig. 9—Latent hardening.

for different orientations of the tensile axis with respect to the crystallographic axes. In terms of the yield locus, these curves show the rate at which those facets of the yield surface that correspond to active slip systems move away from the origin with increasing shear. Nothing is known from such experiments about the other, "latent" systems.

There are two simple assumptions one could make: that the latent systems do not harden at all or that they harden at the same rate as the active systems.<sup>13</sup> Figs. 9(a) and 9(b) show these two cases for two equal increments of strength on the single ("primary") system that yielded first. In case (a), a second system will get activated soon; after one additional equal strength increment, the first system would in fact be deactivated as a third system comes in. The yield surface becomes very anisotropic. In case (b), work hardening is "isotropic": the yield surface blows up like a balloon.

From recent experiments,<sup>9,19-24</sup> it seems that Fig. 9(c) typifies the realistic case: the latent systems harden faster than the active ones; the ratio of the two hardening rates (past easy glide) is roughly constant and at most about 1.4. Latent slip systems on the same slip plane harden at a rate equal to that on the primary slip system.<sup>9,23</sup> (The yield locus in Fig. 9 is a symbolic one, not representing any special class of crystals.) Fig. 9(c) also shows that there may be a Bauschinger effect: the slip system that is the exact opposite of the active one may harden less than the active one.

In polyslip, one may expect little difference between the various active slip systems. Again, the latent systems should harden at an equal or higher rate. In the case of  $\langle 111 \rangle$  compression in aluminum, this has been shown<sup>6</sup> to be the case by alternately compressing and twisting a thin-walled single crystal tube of hexagonal cross section with its axis in the  $\langle 111 \rangle$  direction.

The state of affairs described in Fig. 9(c) is not very different from that postulated by Taylor,<sup>13</sup> Fig. 9(b). Especially under prescribed strain, "isotropic work hardening" is thus a reasonable assumption.

The expanded yield loci shown in Fig. 9 are no different in principle from the original one: if a crystal is unloaded and then reloaded, its new yield criterion is described by the new yield surface. The word "yield strength" is frequently used only for the stress at which a material first becomes plastic. However, since "yield strength" may refer to cold-worked materials as well as to annealed ones, one may regard the stress-strain curve as nothing but the locus of current yield strengths vs (pre-)strain and use the words "yield strength", "yield surface", and so forth, irrespective of whether they are initial or current values.

## Rate Effects

Any influence of strain rate on the yield criterion has been ignored up to now. In the plasticity literature, an assumed absence of rate effects is often stated to be equivalent to a very low strain rate, as if one were close to thermodynamic equilibrium. To achieve a finite strain rate, one would then have to exceed the "rate independent yield surface" by an amount that increases with the rate demanded.

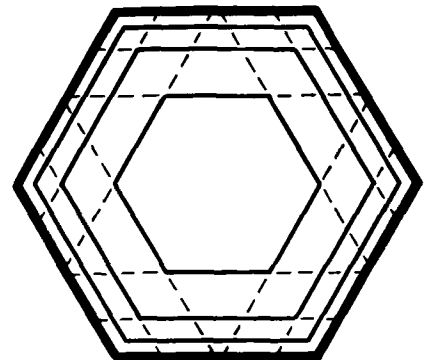
The physical situation is better described as precisely the reverse. Yield is not the consequence of a small deviation from equilibrium; it may rather be called a threshold phenomenon. In all materials, there is a reasonably well defined threshold limiting all elastic states, independent of strain rate, at the absolute zero of temperature. At finite temperature, this threshold gets lowered, in many materials, by thermal activation, and the amount of decrease depends on the strain rate. One may thus define, for any material, a series of yield loci for any combination of strain rate and temperature, all of which are contained within the limiting yield locus for  $T = 0^\circ\text{K}$ . Fig. 10 is a schematic illustration.

If the *stress* is prescribed in a given experiment, rather than the strain rate, one can define a precise elastic limit only at zero temperature. At all finite temperatures, stresses below the limiting yield locus will lead to some finite strain rate which is the lower the lower the stress. In principle, one could thus say that the yield locus for infinitesimal strain rates is a point at the origin. In practice, however, since the strain rates decrease exponentially with the deviation of the stress from the limiting yield locus, there is usually a finite stress at which the testing times would exceed the age of the universe. In this fashion, a yield locus for infinitesimal strain rates would be definable, although it would be less useful than the one for zero temperature.

Fig. 10 also shows an interesting effect which bears on the basic tenet of the Schmid law: that only those systems may be operative for which the "yield strength" is reached. Evidently, slip systems other than the most highly stressed one will, in this picture, provide some strain rate, although it will be lower than that on the primary system. In practice, these strain rates may again be vanishingly small, but this depends on the deviation of the applied stress from edges of the yield surface, and on the detailed model of strain rate sensitivity.

In the remainder, we shall ignore strain rate and temperature effects.

Fig. 10—The "rate independent" yield surface, *i.e.*, the one for absolute zero temperature. Inside it (—) the yield surfaces for increasingly lower strain rates. The extensions (---) allow for different strain rates on different slip systems.





## THE THEORY OF POLYCRYSTAL DEFORMATION

We shall only deal with plastic deformation, not with fracture. Since the absence of sufficient modes of plastic deformation may lead to premature fracture, there is a significant interaction between the two fields. Some general observations on this relationship are contained in a paper dealing with the specific case of cph materials.<sup>25</sup>

We shall also restrict ourselves to homogeneous deformation throughout a specimen (or a sufficiently large part of it to qualify as a "polycrystal"), and exclude cases in which the macroscopic strain gradient is significant on the scale of the grain size, whether by virtue of external boundary conditions or as a result of the particular deformation mode of the material.

### Elasto-Plastic Solutions

A polycrystal in the ideal sense defined in the first section contains very many grains of the same orientation (within a certain small range), each one of which has a different set of surrounding grains. Since we assume no correlation between the orientations of neighboring grains, all these surrounding grains taken together are a large random set and are as isotropic as the whole polycrystal is assumed to be. For this reason, one may average out the effect of the surroundings on the grains of any particular orientation. Kröner<sup>26,27</sup> proposed a model, illustrated in Fig. 11, in which all grains of one crystallographic orientation (within a certain small range) are represented by a single spherical grain, and the surrounding matrix is represented by an isotropic continuum. This case itself may then be treated by the Eshelby<sup>28</sup> method, and subsequently averaged over grains of all orientations.

The Eshelby method may be described by the following thought experiment. First, the spherical or ellipsoidal grain is cut out of the isotropic matrix. When surface tractions are applied to the matrix at infinity, which give rise to the macroscopic average stress  $\bar{\sigma}$ , surface tractions are applied at the hole such that the surrounding material is under the same stress state as it would be if the hole were filled with the isotropic continuum also. The matrix will then deform elastically and plastically in a certain uniform way; the plastic strain of the hole may be described by  $\bar{\epsilon}$ . (The *elastic* strains in matrix and grain are assumed to be identical. For a consideration of *elastic* anisotropy also, see Hook and Hirth<sup>29</sup> and Willis.<sup>30</sup>) Now the surface

tractions that had to be applied to the inside surface of the hole are applied, with opposite sign, to the separated grain. Presume that these surface tractions will make the grain yield and give rise to a plastic strain  $\epsilon$ . (All the  $\sigma$ 's and  $\epsilon$ 's are tensors.) If one now wants to insert the grain back into the matrix, it will not fit: the "compatibility conditions" have been violated. From this point on, both grain and matrix are treated as elastic,\* and a distribution of in-

\*This inconsistency has also been pointed out by Hill<sup>31</sup> who gave a more general solution.

ternal stresses and elastic strains is found that will make the grain fit back into the hole. As Eshelby<sup>28</sup> has shown, the internal stress is uniform inside any grain of ellipsoidal shape, and it is directed precisely opposite to the difference between the plastic strains of grain and hole. In other words, some of the plastic strain is undone elastically. Let  $\sigma$  be the total stress inside the grain. Then, according to Kröner,<sup>27</sup>

$$(\sigma - \bar{\sigma}) = -\alpha G(\epsilon - \bar{\epsilon}) \quad [19]$$

where  $G$  is the appropriate elastic modulus and  $\alpha$  is a scalar constant of order  $\frac{1}{2}$ .

Regardless of any quantitative details, we may conclude from Eq. [19] that the differences in strain (both magnitude and direction) between neighboring grains cannot be very large: a difference of a few percent would cause fracture, and many yield mechanisms may intervene before that.

There are two basically distinct modes of yield that may occur in response to the attempt by any grain to deform by an especially large amount. One is by a chain reaction in which neighboring grains yield under the forward stress concentration caused by the yield of the previous grain. If this mechanism proceeds through an entire cross section, it leads to the formation of a Lüders band. Since the stress concentration from the first grain falls off with a characteristic distance of the order of the average grain diameter, the second grain would deform to a significant extent only if yield is controlled by the generation of dislocations rather than by their propagation through the entire grain.

The other mode of yield, with which we shall deal exclusively from here on, consists of the activation of additional slip systems in the first grain, through the action of the internal stress, Eq. [19].

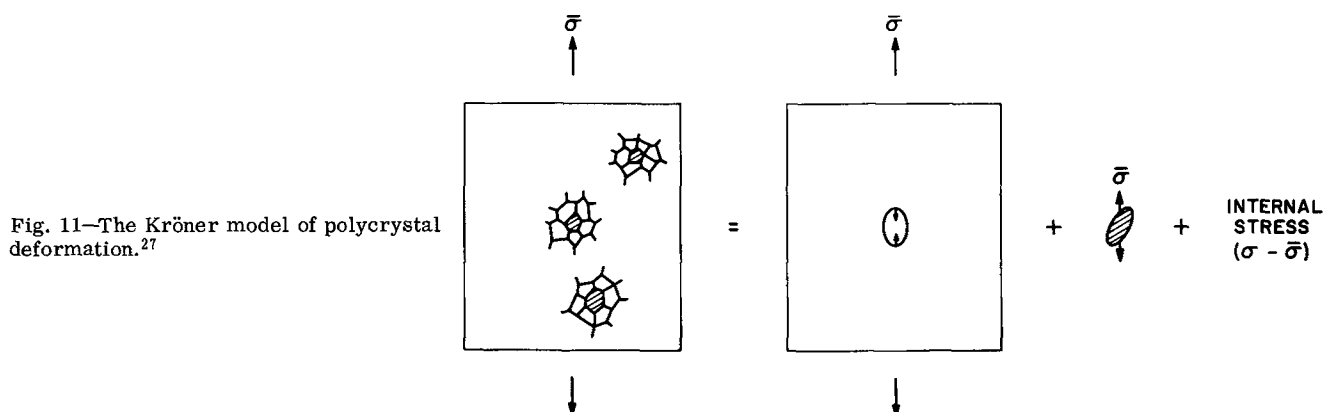


Fig. 11—The Kröner model of polycrystal deformation.<sup>27</sup>

The mechanism by which the transition from single slip to multiple slip occurs, may be shown in a sketch of a typical yield surface, Fig. 12. For simplicity, let us first neglect work hardening and treat the case where the plastic strain in the matrix  $\bar{\epsilon} = 0$ , in the right hand part of the figure. When the applied stress  $\bar{\sigma}$  first reaches the yield surface, the strain  $\epsilon$  would be described by an arrow pointing vertically upward. The internal stress ( $\sigma - \bar{\sigma}$ ) inside the grain would then be represented by an arrow pointing vertically down. If the grain is to continue to deform, the total stress  $\sigma$  in the grain must be located on the yield surface; thus  $\bar{\sigma}$  has to be raised to the first level shown by an arrow.

It is seen that the stress state in this grain moves away from the normal to the facet of the yield surface that corresponds to the first active slip system. After a little further strain and stress increase, it has reached an edge of the yield surface and the second slip system is activated. If the stress state is still not contained in the fan of normals of this edge, it will move along the edge, in the direction away from the origin, and will soon arrive at another "edge" where three systems meet. By this procedure, the stress

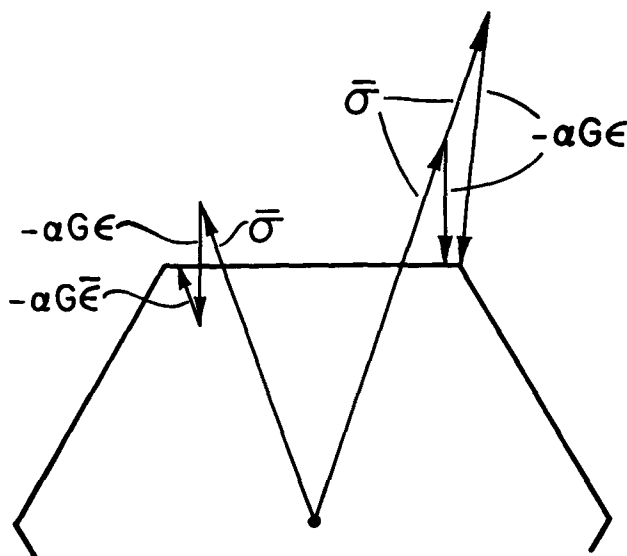


Fig. 12—Series of applied and internal stress states during the elasto-plastic transition region, shown on a typical yield locus section.

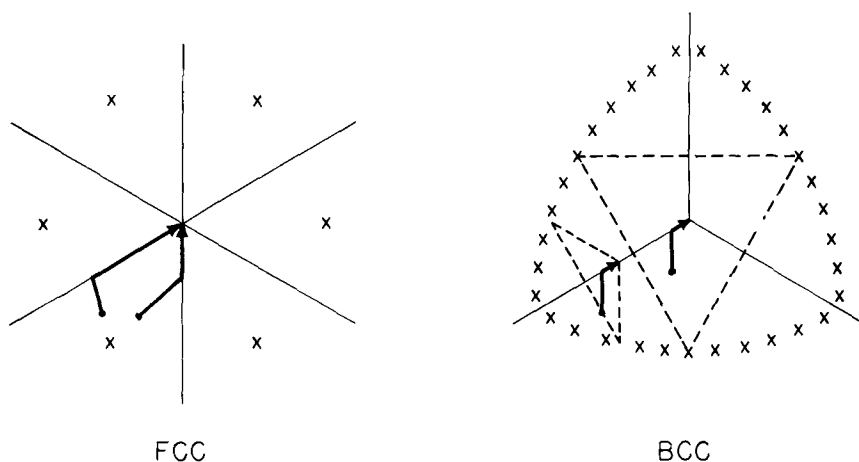


Fig. 13—Stress paths under prescribed strain. In the example, view in the Z-direction of the yield surfaces shown in Figs. 3 and 8, respectively.  $\times$  marks points at which normals to the yield surface from the origin emerge.

state eventually has to end up in the "corner" of the yield surface whose cone of normals does contain the stress vector.

Fig. 13 shows two such paths for two different initial stress states in a view of the fcc yield surface that could, for example, be in the Z direction of Fig. 3 ( $\langle 111 \rangle$  tension). In this particular case, the number of activated slip systems jumps from two to six. Fig. 13 also shows the equivalent situation, for the same two initial stress states, in bcc pencil glide (e.g., the view in the Z direction of Fig. 8, again  $\langle 111 \rangle$  tension). Since the direction of the fan of normals continuously changes along the curved edges of this yield surface, the stress state may be contained in a 2-dimensional fan of normals before it reaches the 3-dimensional fan that looks like a corner in Fig. 13. In the case shown in the figure, only those stress states that are contained within the dashed triangle will eventually activate three slip directions.

On the left-hand side of Fig. 12, the effect of a finite matrix strain  $\bar{\epsilon}$  is incorporated with the assumption that it is parallel to  $\bar{\sigma}$ . In this case, the approach to the first edge is even more rapid. In either case, the amount of plastic strain occurring before the stress state reaches the proper corner of the yield surface is of the order of magnitude of the elastic strain at yield. Only when  $\bar{\sigma}$  is very close to the pure shear stress necessary to activate one slip system may the strain be much larger. Both Payne<sup>32</sup> *et al.* and Budiansky and Wu<sup>33</sup> have come to this conclusion from different but equivalent<sup>34</sup> studies on fcc grains of many orientations. They have found that, even in the average, the strain at which the final corner has been reached is no more than a few times the elastic strain at yield. At about 1 pct strain, the distribution of strains should thus be quite uniform.

If the yield surface expands through work hardening during these loading experiments, the approach of the stress state to a corner of the yield surface will be slower.\*<sup>34</sup> However, even heavily work hardened ma-

\*The stress state would stop changing "direction" when the tangent to the work hardening curve goes through the origin—an unrealistic case.

terials rarely take elastic strains of the order of 1 pct, an amount still negligible with respect to the plastic strains.

According to these results, a grain imbedded in a polycrystal thus behaves as if the strain it has to produce were prescribed by its surroundings and were

indeed very similar to the macroscopic average strain (Eq. [19]). This is the basic hypothesis for polycrystal deformation advanced by Taylor<sup>13</sup> in 1938.

For the case of the *elastic* deformation of polycrystals, the assumption of uniform strain had been used previously by Voigt.<sup>35</sup> Reuss,<sup>36</sup> on the other hand, assumed uniform *stresses*, and he averaged over the strains.

Hill<sup>37</sup> has shown that any method in which the compatibility conditions are fulfilled although the equilibrium conditions may be violated gives an upper bound for the elastic moduli of the polycrystal, whereas any method in which the equilibrium conditions are fulfilled (although the compatibility conditions may be violated) gives a lower bound. For realistic degrees of anisotropy, the arithmetic average between these two bounds is often a sufficiently accurate solution to the problem of an elastic polycrystal.

Similarly, the assumption of uniform strain in a plastic polycrystal strictly gives an upper bound for the yield stress,<sup>38,39</sup> and an assumption of uniform stress would give a lower bound. In this sense, Taylor's model of polycrystal deformation presupposes that, in the case of plasticity, the upper bound is much closer to the true solution than the lower bound. With the help of the elasto-plastic solutions discussed above (Eq. [19]), one can easily see why this should be so.

When the strains are large, compatibility is especially important. Satisfying compatibility trivially by assuming the strains to be uniform generally violates equilibrium conditions across the grain boundaries. This is particularly obvious in our case of single crystals with faceted yield surfaces: any arbitrary strain generally demands one of a small number of discrete stress states that are very unlikely to be in equilibrium across any grain boundary. However, this situation may be amended by superimposing an internal stress field designed to satisfy equilibrium conditions everywhere. The elastic strains associated with this internal stress field may now, in general, destroy the previously satisfied compatibility conditions. The crux of the argument is that such elastic strains are always small compared with any plastic strains of interest and should thus not influence the compatibility condi-

tions appreciably. Budiansky and Wu<sup>33</sup> have shown that "large plastic strains" in this connection are plastic strains larger than about five times the elastic strain, or about 0.1 pct.

### The Taylor Model

In the original Taylor<sup>13</sup> proposal, elastic strains were neglected and the strain in each grain was set exactly equal to the macroscopic average strain:

$$d\epsilon = d\bar{\epsilon} \quad [20]$$

Inasmuch as volume strains cannot be imposed onto such a plastic-rigid material, five independent slip systems are necessary to satisfy any arbitrary prescribed strain.<sup>40</sup> All possible combinations of five slip systems in fcc crystals (with the exception of some left out by mistake, as has been frequently pointed out<sup>41</sup>) were then considered by Taylor; among them he selected any one of the combinations giving the lowest algebraic sum of shears, using a hypothesis based on an analogy with sliding rigid bodies.

The necessity of fulfilling the yield criterion was not recognized: a stress state has to exist which activates all the slip systems selected in the proper direction and which does not exceed the flow stress on any other (positive or negative) slip system. We shall now show that Taylor's minimum shear sum criterion is in fact equivalent to fulfilling the yield condition.\*

\*Note added in proof: This equivalence has now also been shown, in a different way, by Chun and Mammel.<sup>41a</sup>

Let a given prescribed strain increment  $d\epsilon$  be resolved, Fig. 14(a), into two different sets of five independent slip systems, a "wrong" one ( $s$ ) and a "right" one ( $\tilde{s}$ ), resulting in the shears  $d\tilde{\gamma}^{\tilde{s}}$  and  $d\gamma^s$ , respectively:

$$d\epsilon_\nu = m_\nu^{\tilde{s}} d\tilde{\gamma}^{\tilde{s}} = m_\nu^s d\gamma^s \quad [21]$$

Now consider the stress  $\tilde{\sigma}$  that would activate every one of the systems  $\tilde{s}$  in the correct direction demanded by Eq. [21], so that (Eq. [1a])

$$\tilde{\sigma}_\nu m_\nu^{\tilde{s}} = \tau^{\tilde{s}} \quad (\nu = 1, \dots, 6) \quad [22a]$$

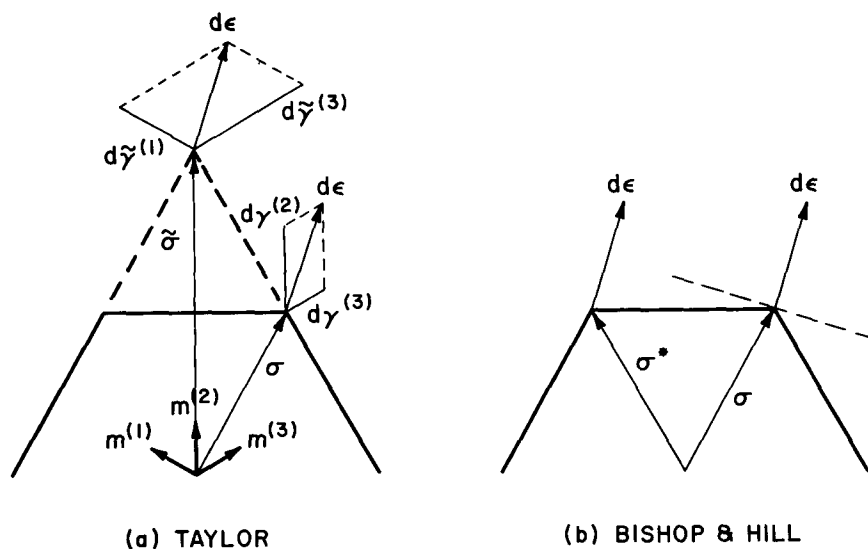


Fig. 14—Two methods of finding the proper slip system combination for a given strain  $d\epsilon$ : (a) the combination with the larger sum of shears violates the yield condition; (b) the wrong corner of the yield surface does not contain  $d\epsilon$  in its cone of normals. (a) is a minimum work criterion, (b) a maximum work criterion.

This same stress  $\tilde{\sigma}$  may exceed the yield stress in some systems not in the set ( $\bar{s}$ ). Let us specifically assume that  $\tilde{\sigma}$  exceeds the yield stress in at least one of the systems  $s$  belonging to the "right" set, so that

$$\tilde{\sigma}_\nu m_\nu^s > \tau^s \quad [22b]$$

Scalar multiplication of  $\tilde{\sigma}$  into Eq. [21] shows that

$$\tilde{\sigma}_\nu d\epsilon_\nu = \tilde{\sigma}_\nu m_\nu^s d\tilde{\gamma}^s = \tilde{\sigma}_\nu m_\nu^s d\gamma^s \quad [23a]$$

and, with Eqs. [22a] and [22b],

$$\tau^s d\tilde{\gamma}^s > \tau^s d\gamma^s \quad [23b]$$

Assuming an isotropic flow stress (Eq. [11]), we get

$$\sum_s \tilde{\gamma}^s > \sum_s \gamma^s \quad [23c]$$

As we set out to demonstrate, the algebraic sum of shears is larger for the combination of slip systems that violates the yield condition. If two combinations can be found both of which can provide the macroscopic strain without violating the yield condition, the algebraic sum of shears is equal in the two combinations, as one could already have deduced from Eq. [15].

Eq. [23b] says that the correct combination of slip systems requires the least work. It is important to note, however, that this "minimum work" criterion is a strictly geometric one and bears no relation whatever to any thermodynamic principle. This point becomes even more evident when one considers an alternative method to select the proper corner of the yield surface, derived by Bishop and Hill,<sup>42</sup> which leads to a "maximum work principle".

Since an arbitrary prescribed strain state requires a corner stress state, one could try out each corner of a given yield surface (56 in the case of fcc crystals) instead of the many more combinations of five slip systems out of twelve even after dependencies have been eliminated. However, a criterion would be needed to specify which corner is the proper one. Such a criterion was derived by Bishop and Hill<sup>42</sup> and is illustrated in Fig. 14(b). The stress into the "right" corner is called  $\sigma$ , the stress into a "wrong" corner is called  $\sigma^*$ . The "right" corner may be characterized as being the one which would be first touched by a plane perpendicular to  $d\epsilon$  that is brought in from infinity. In algebraic form,

$$\sigma_\nu^* d\epsilon_\nu < \sigma_\nu d\epsilon_\nu \quad (\nu = 1, \dots, 6) \quad [24]$$

In other words, the "right" stress state does the *larger* work. It all depends on what is varied.

By either method, one may thus derive the proper Taylor factors  $M$  for each orientation. Taylor<sup>13</sup> averaged\* these  $M$  factors over all orientations and re-

\*For a general discussion of the subtleties involved in averaging tensor quantities, see Hill.<sup>43</sup>

lated the yield stress  $\sigma_0$  of polycrystals in tension to the glide yield stress  $\tau_0$  by

$$\sigma_0 = \bar{M} \tau_0 \quad [25]$$

For fcc crystals, he found

$$\bar{M} = 3.06 \quad [25a]$$

Eq. [25] follows from Eq. [17] if one assumes that  $\tau_0$  is the same in all grains of an annealed polycrys-

tal, which implies that the work hardening experienced by those grains which were first to yield is negligible.

## Work Hardening

Taylor<sup>13</sup> assumed the flow stress to be isotropic not only in annealed crystals, but also after work hardening has taken place. In polyslip, this is not an unreasonable assumption as was discussed in the preceding section. A logical extension, also proposed by Taylor,<sup>13</sup> is to make this flow stress depend only on the algebraic sum of shears:

$$\tau = \tau(\Gamma) \quad [26]$$

Although  $\tau(\Gamma)$  is certainly not the same for free single crystals of all orientations, Eq. [26] may be correct under true polyslip conditions.\* To convert

\*In dislocation language, this can be expressed as follows: Isotropic flow stress means that the flow stress depends on the average dislocation density  $\rho$  only. Isotropic work hardening means that the dislocation mean free path  $L^2$  in  $d\rho = d\gamma^s/bL^2$  is the same for each slip system ( $s$ ). Thus  $d\tau^2 \propto d\rho \propto [1/bL(\tau)] \cdot d\Gamma$

the single-crystal  $\tau(\Gamma)$  curve into the polycrystal tensile stress strain curve, Taylor then set

$$\bar{\sigma} = \bar{M} \tau(\bar{\Gamma}) \quad [27a]$$

and

$$\bar{\Gamma} = \bar{M} \bar{\epsilon} \quad [27b]$$

Eq. [27b] is exactly correct from Eq. [15] in Taylor's model of uniform strain (Eq. [20]). The finite opening angle of the cones of normals of the yield locus corners shows, however, that such a stringent condition was not necessary. If one allowed the strain to vary a bit from grain to grain, to the extent allowed by Eq. [19], one would generally still activate the same corner and thus get the same  $M$ . Only the demarcation lines between different corner states (Fig. 5) would be somewhat washed out. There should still be little if any correlation between  $M$  and  $d\epsilon$  since  $d\epsilon$ , in this model, is prescribed by the *surroundings* of each grain, whereas  $M$  is a function only of the orientation of the grain itself. In the absence of such correlations, Eq. [27b] is correct.

Eq. [27a], on the other hand, presupposes that there is no correlation between the orientation of a grain and its flow stress. This is in direct contradiction to the assumption of an essentially uniform strain  $\epsilon$ , which implies different shear sums for different orientations and therefore different flow stresses (Eq. [26]).

In general, one should express the work-hardening law in differential form, with a stress-dependent work-hardening rate  $\theta$ :

$$d\tau = \theta d\Gamma \quad [28a]$$

Then it is generally true that

$$d\bar{\sigma} = M d\tau = \bar{M} \theta d\bar{\Gamma} = \bar{M}^2 \theta d\bar{\epsilon} \quad [28b]$$

where the bar denotes the average over all orientations. If one assumes *essentially uniform strain*, *linear work hardening* ( $\theta = \text{const.}$ ) and *negligible yield stress*, one finds

$$d\bar{\sigma}/d\bar{\epsilon} = \bar{M}^2 \theta \quad [29a]$$

On the other hand, Taylor's Eqs. [27] would have given, under the same conditions,

$$d\sigma/d\epsilon = \bar{M}^2 \theta < \bar{M}^2 \theta \quad [29b]$$

In reality, Taylor's formula is probably not bad. The work-hardening rate  $\theta$  generally decreases with increasing  $\Gamma$ ; since grains with a high  $M$  have a high  $\Gamma$ , under essentially uniform strain conditions, there should be an inverse correlation between  $\theta$  and  $M$ . Furthermore, any correlation that might exist between the strain increment  $d\epsilon$  of a particular grain and its orientation should make  $\epsilon$  smaller for harder grains, *i.e.*, for high  $M$ . Both considerations would tend to lower  $d\bar{\sigma}/d\bar{\epsilon}$  from the value given in Eq. [29a], possibly approaching that given in Eq. [29b].

In any case, Eqs. [25] and [29a] provide an upper bound for the flow stress of polycrystals according to the Taylor model—which, as we have seen, is itself an upper bound to the correct solution of the polycrystal problem in general.

Any deviation from the assumptions leading to Eq. [29a], namely linear work hardening and negligible yield stress, has one further consequence: any curvature in the  $\tau(\Gamma)$  diagram will reappear *less strongly curved* in the  $\bar{\sigma}(\bar{\epsilon})$  diagram. This is due to the fact that, at any given strain  $\epsilon$ , there will be a spread of  $\Gamma$ 's in the grains by roughly a factor 2. Thus, the polycrystal takes a moving average over a certain *range* of the single crystal curve. In the elasto-plastic transition region of a material with a *finite* yield stress and linear work hardening, this effect has been treated quantitatively by Hutchinson.<sup>34</sup>

#### The Yield Locus of Polycrystals

The presumed isotropy of a "polycrystal" limits the range of possible yield criteria, but it does not uniquely determine any particular one. Two hypotheses are in common use for phenomenological purposes: the Tresca<sup>45</sup> criterion according to which the maximum shear stress in the body has to reach a critical value for yield; and the von Mises<sup>46</sup> criterion according to which the second invariant of the stresses has to reach a critical value. Application of the "associated flow rule" (Eq. [6]) to the Tresca criterion predicts a pure shear strain at yield, irrespective of the nature of the applied stress; combination of the "associated flow rule" with the von Mises yield criterion makes the strain increments parallel to the (deviatoric) applied stress.\*

\*This proportionality between each component of the strain rate and the respective nonhydrostatic stress component does not follow from isotropy, and it does not follow from (reversible or irreversible) thermodynamics. Claims to the contrary<sup>47,48</sup> disregard the essential nature of threshold phenomena, as opposed to small deviations from equilibrium (or a kinetic balance) in a parabolic potential.

From a physical point of view, the Tresca criterion should apply in the following two cases:<sup>49</sup> yield of the first grain in a polycrystal, if this were ever observable; and macroscopic yield in the Lüders mode, when stress concentrations due to the first operative grain trigger the spreading of slip. Indeed, the Tresca yield criterion has consistently been observed to hold fairly well in materials that show a yield drop.<sup>50</sup>

A minimal condition for the von Mises yield criterion to apply is that slip should occur in all directions in which there is any shear stress, *i.e.*, in *all* directions. Even in polyslip, however, the five or even eight operative slip systems will cluster around the di-

rection of maximum shear stress and will be absent in planes and directions nearly parallel to the principal axes of stress. One should thus expect a deviation of the observed yield surface from the von Mises hypothesis toward the Tresca hypothesis. Observations on materials that yield by homogeneous plastic flow are indeed generally observed to obey the von Mises criterion or to deviate slightly from it in the predicted direction.<sup>48,51-53</sup>

Bishop and Hill,<sup>42</sup> who derived the Taylor factor for polycrystal tension with the same result as Taylor<sup>13</sup>, have also applied the polyslip model to other stress states. For pure shear, for example, they find  $\bar{M} = 1.65$ , as compared to  $\bar{M} = 3.06$  in tension. For the same value in tension, the von Mises criterion would have made the shear constant 1.77 ( $= 3.06/\sqrt{3}$ , see *e.g.* Hill<sup>51</sup>), the Tresca criterion would have made it 1.53 ( $= 3.06/2$ ).

It should be remembered that the polyslip model applies to the fully plastic state. The yield stress should thus be defined by the back extrapolation of the stress-strain curve to zero plastic strain, not by any prescribed deviation from straight-line elastic behavior.

Upon reloading a prestrained polycrystal in the reverse direction, one frequently observes a Bauschinger effect that is distinct from that observed in single crystals. Hutchinson<sup>34</sup> has explicitly obtained the theoretical result, based on the Kröner<sup>27</sup> model, that the proportional limit in reverse straining should be severely reduced (or even become negative), although the yield stress defined by back extrapolation is the flow stress last observed during forward straining.

#### Application to bcc Crystals

We have seen that bcc crystals which slip on  $\{110\}$  planes have a yield surface identical to that of fcc crystals. Thus, the average Taylor factor must be the same:  $\bar{M} = 3.06$ .

For pencil glide, Taylor<sup>54</sup> had outlined a program that could not be executed before the advent of computers, but has since been done in approximate fashion by Hutchinson<sup>55</sup> and by Chin and Mammel.<sup>56</sup> They found

$$\bar{M} \approx 2.75 \quad [30]$$

A lower limit for this  $\bar{M}$  in pencil glide is, however, very easily derived by the use of the yield surface and the Bishop and Hill variation method. In the foregoing, we have seen that the bcc pencil glide yield surface can be derived from the fcc yield surface by replacing various hexagonal cylinders with circular cylinders. Some of the edges vanish in this procedure, and the corners in the fcc yield surface become "edges" where three or four slip directions are simultaneously activated. The "maximum work principle" (Eq. [24]) introduced by Bishop and Hill<sup>42</sup> and illustrated for this case in Fig. 15, enables one to get the lower limit for  $\bar{M}$  in each grain by falsely assuming that all grains in bcc polycrystals deform with the stress states corresponding to the corners in the fcc yield surface. The distance of all these corner stress states from the origin is now equal to  $\frac{1}{2}\sqrt{3}$  times the respective distance in the fcc yield surface. Thus,<sup>57</sup>

$$\bar{M} > \frac{1}{2}\sqrt{3} \cdot 3.06 \approx 2.65 \quad [31]$$

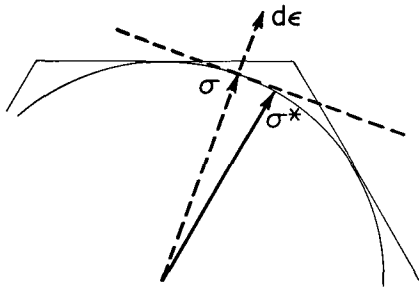


Fig. 15—Application of Bishop and Hill's<sup>42</sup> maximum work principle to pencil glide.

$$(\sigma - \sigma^*) d\epsilon \geq 0$$

For all physical situations of approximate pencil glide where the  $\{110\}$  plane may be somewhat preferred, the average Taylor factor has to lie between 2.65 and 3.06. If, for pencil glide, one uses the value 2.75 derived numerically by Hutchinson<sup>55</sup> and by Chin and Mammel,<sup>56</sup> one may write

$$\bar{M} = 2.9 \pm 5 \text{ pct} \quad [31a]$$

irrespective of slip mode.<sup>57</sup>

An interesting prediction concerning slip line observations may also be derived from the pencil glide yield surface. We have seen in Fig. 14 that most grains will never reach a state in which three or four slip directions are activated simultaneously—yet more grains reach these stress states than any other *specific* stress state. These symmetric stress states have one characteristic in common, namely that the slip plane of maximum resolved stress is always the crystallographic  $\{211\}$  plane.\* Thus one should expect to ob-

\*This is the equivalent of the observation that, in fcc corner stress states, two  $\langle 110 \rangle$  slip directions are activated in every  $\{111\}$  slip plane

serve a marked tendency for  $\{211\}$  slip lines on polycrystals of materials which, as single crystals, show essentially pencil glide.<sup>57</sup>

### The Development of Deformation Textures

We have seen that all corners in the yield surface for crystallographic slip allow additional arbitrary rotations. These rotations are restricted to a single axis in those cases where six slip systems are activated. In the particular case of tension in fcc materials, the allowed arbitrary rotation is a twist around the tension axis and thus does not lead to any change in a fibre texture. Furthermore, it is due to strong differences in the amounts of slip obtained in two different directions on the same slip plane; latent hardening experiments of single crystals suggest that this is not likely to occur. In tension or compression, those fcc grains with orientations in the upper part of the stereographic triangle shown in Fig. 5 should thus rotate in a well prescribed direction.

In those polyslip states where eight slip systems are activated (the three regions touching the  $\langle 100 \rangle$ - $\langle 110 \rangle$  line in Fig. 5), additional rotations are entirely arbitrary. The direction in which these grains rotate is thus determined by which particular combination of five or more slip systems is in fact operative, although they all give the same algebraic sum of shears.

Taylor<sup>13</sup> assumed that exactly five systems would

operate and thus made an inherent assumption on latent hardening. Furthermore, he was arbitrary in the selection of the particular combination of five systems presumed operative. Finally it is possible that those states which Taylor failed to consider,<sup>41</sup> although they did not influence the result on  $\bar{M}$ , would have affected the deformation textures he predicted in a more sensitive way. It is thus not surprising that the deformation texture derived by Taylor was not particularly successful.

To derive a better deformation texture, which allows for variations from one material to another under the same configuration of potential slip systems, one will have to incorporate a realistic hypothesis about latent hardening into the theory. In general, isotropic hardening will tend to give a uniform distribution of slips over all activated slip systems, whereas high latent hardening will tend to give slip on as few systems as possible. An assumption in this general direction was made in a qualitative paper by Bishop.<sup>58</sup> Lin and Lieb<sup>59</sup> used a hypothesis that has since gained substantial experimental support,<sup>9,23</sup> Fig. 9, namely that intersecting slip planes harden more, whereas systems in parallel planes harden at the same rate.

Experimentally observed deformation textures in fcc materials fall into two classes which have been correlated with the stacking fault energy of the material.<sup>60,61</sup> It is indeed conceivable that the stacking fault energy influences latent hardening directly. Alternatively, high stacking fault energy could lead, at high strains, to deformation by essentially pencil glide, thus altering the yield surface. Finally, latent hardening may depend on whether the deformation occurs in stage II or stage III of work hardening and this depends, at a given strain, on the stacking fault energy. Detailed experiments are necessary to ascertain which of the physical mechanisms is at the root of the observed spread in deformation textures.

The application of the model to the deformation of bcc materials allows one to make one statement concerning deformation textures the truth of which is self-evident and even confirmed by experiment: when slip plane and slip direction are interchanged, the macroscopic strain stays the same but the rotation changes sign;<sup>14</sup> thus the compression texture of bcc should be equal to the tension texture of fcc and vice versa.

If bcc crystals deform by pencil glide, there are no corners left in the yield surface in which there is any ambiguity in the decomposition of the applied strain into the various slip systems.<sup>18</sup> Thus the deformation texture should be unique for bcc materials. This is again in good agreement with fact.

### The Sachs Model

The oldest model of polycrystal deformation is that proposed by Sachs<sup>62</sup> in 1928 and again, in slightly altered forms, by Cox and Sopwith,<sup>63</sup> Kochendörfer<sup>41,64</sup> and, most recently, by Schwink and coworkers.<sup>65,66</sup> In the form given by Kochendörfer, it predicts, instead of Eqs. [27], for a uniaxial test in the z-direction:

$$\sigma_{zz} = \sigma_0 + \overline{1/m} \cdot \tau(\gamma_p) \quad [32a]$$

$$\gamma_p = \overline{1/m} \cdot \epsilon_{zz} \quad [32b]$$

where  $\tau(\gamma_p)$  is a stress strain curve typical of single slip on the primary or most favored system in free single crystals, and  $m$  is the Schmid factor defined in Eq. [2a], the average for fcc crystals being<sup>62,63</sup>

$$\overline{1/m} = 2.238 \quad [33]$$

This result would be obtained<sup>67</sup> if one assumed a series of parallel but free single crystals: the tensile strain in the  $z$ -direction would be the same for every grain, although all other components of strain would be different from grain to grain. The tensile stress would be different from grain to grain, but all other stress components would be zero in each grain. Such an arrangement would fulfill equilibrium and yield conditions but would violate compatibility conditions. By the arguments given earlier, the model should thus provide a lower bound for the polycrystal stress strain curve, and should become a progressively worse approximation the larger the plastic strain.

The additional constant contribution  $\sigma_0$  to the flow stress (Eq. [32a]) was introduced by Kochendörfer<sup>41</sup> to account for internal stresses set up by the incompatibilities. We have seen in Eq. [19] that such internal stresses would become much too large to be presumed to be of no consequence to the basic deformation mechanism. Furthermore, as Masing<sup>68</sup> has pointed out, the model would demand that all work done against  $\sigma_0$  be stored—which is far beyond the range of possibilities allowed by the experiments.

The chief argument used in favor of the Sachs model is based on metallographic observations of essentially single slip in any particular region on the surface of a deformed polycrystal, so long as it is not in the immediate vicinity of a grain boundary.<sup>65,66,69</sup> There are a number of experimental flaws in such observations. Firstly, the surface grains are not under the full constraint of the compatibility conditions caused by the interaction of grains across grain boundaries. Secondly, *one* observed slip line may, and often does,<sup>70,71</sup> correspond to *two* independent slip systems. Thirdly, even under the conditions of polyslip, one would rarely expect roughly equal amounts of glide on all active slip systems; the plane that predominates may well show up even more exclusively in light microscope pictures.

These difficulties may be minimized by the careful use of electron microscope replica and transmission techniques.<sup>71</sup> In many cases, the most realistic characterization of the slip distribution in polycrystals may in fact be a segmentation of grains into domains in which a single slip system or a single slip plane predominates, but different systems in different domains of the same grain. Even in such a case, though, Eqs. [32] would not describe the polycrystal stress strain curve.

The conditions of compatibility have to be satisfied for *any* volume element in the body, for domains as well as for grains. Single slip in domains leading to the formation of stress-free small-angle boundaries is thus not possible.

Furthermore, the averaging procedure prescribed in Eqs. [32] presumes that in each grain only one slip system operates: *the one with the highest resolved shear stress*. The fundamental reason why  $\overline{M}$  in Eqs. [27] is higher than  $\overline{1/m}$  in Eqs. [32] is that some less favored slip systems have to operate, too. Even when

the less favored systems operate in concentrated form in smaller regions, they still have to have a high enough resolved stress.

We are thus forced to conclude<sup>67</sup> that the basis for the Sachs model is theoretically unsound. There is no reason why one should ever use<sup>71</sup> an “average orientation factor” that is the mean of the Sachs and Taylor values.

By contrast, we may summarize that the various objections raised against the Taylor model proved to be directed against specifics of the original proposal and not against the substance of the model itself. The strain is indeed not uniform from grain to grain; yet the sharp corners in the single crystal yield surface allow substantial deviations without affecting the results. The yield condition had not even been considered; yet it was fulfilled by an ad hoc hypothesis. Neither the flow stress nor the work hardening rate are the same in all active slip systems; yet they are in fact much more closely the same than had long been thought. The predicted deformation texture did not fit the experiments well; yet the specific arbitrary assumptions made by Taylor to derive this result may be replaced by more realistic ones without affecting the rest of the theory.

One cannot help but marvel at the foresight contained in Taylor's work of the 1930's, and one may wonder how the field would have progressed had his rather crude determinations of stress strain curves not happened to “substantiate” the theory.

## EXPERIMENTS

### Stress Strain Curves

Figs. 16 and 17 show shear stress vs shear curves for typical single crystals of iron and aluminum, respectively. Most single crystals of random orientations would show curves roughly similar to the “single slip” curves in Figs. 16 and 17, for which the Schmid

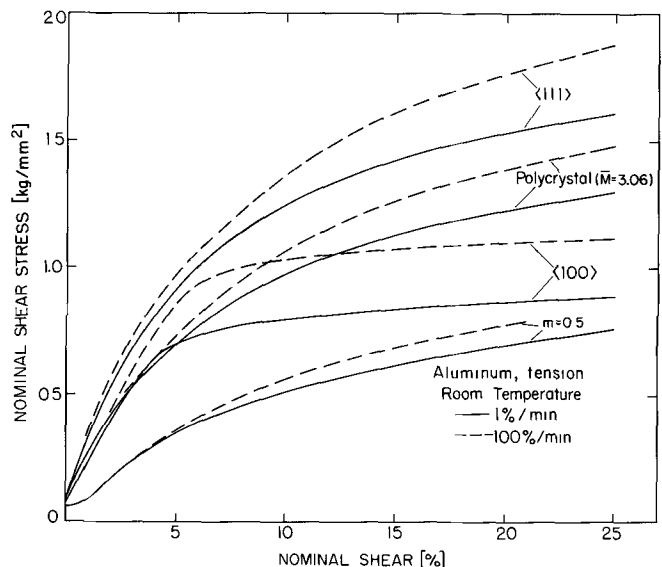


Fig. 16—Nominal stress strain curves (without correction for area changes and orientation changes) for 99.99 pct pure Al, at two tensile strain rates: three single crystals of different orientations and one polycrystal of a grain size of 0.2 mm (15 pct surface grains). After Kocks *et al.*<sup>72</sup>

factor  $m = 0.5$ . The two corner orientations  $\langle 100 \rangle$  and  $\langle 111 \rangle$  are included in the figures because of their particular relevance to polycrystal deformation. Polycrystal curves for these two materials are also shown on the figures, converted to shear stress and shear sum by Taylor's Eqs. [27] with  $\bar{M}$  values according to Eq. [25a] for crystallographic slip in aluminum, and according to Eq. [30] for pencil glide in iron.

Figs. 16 and 17 demonstrate that the difference in work-hardening behavior between different single crystal orientations far outweighs in importance the subtleties of averaging discussed in the last section. The most striking feature of single crystal work hardening is that intersecting slip systems interact strongly, so that polyslip is harder than single slip. It makes no sense, therefore, to compare the polycrystal with the *average* single crystal in free tension; instead one should<sup>10</sup> compare the polycrystal with single crystals deforming in polyslip.\*

\*The orientation dependence of less pure single crystals, such as the aluminum used by Taylor,<sup>13</sup> is much weaker; the problem did thus not exist then.

Indeed, the polycrystal curve falls between the  $\langle 100 \rangle$  and  $\langle 111 \rangle$  curves in both materials. Specifically, easy glide is absent in all, the yield strength is similar, and so is the rapid hardening in stage II. Dynamic recovery in stage III is quite different for single crystals of different polyslip orientations,<sup>12</sup> for reasons that are not well understood. In some cases, such as in single crystals of  $\langle 100 \rangle$  orientation in aluminum, symmetric stress states do not in fact produce polyslip in free single crystals, and the rapid saturation of the  $\langle 100 \rangle$  stress strain curve may be connected with this effect.<sup>12</sup> It is then not surprising that the

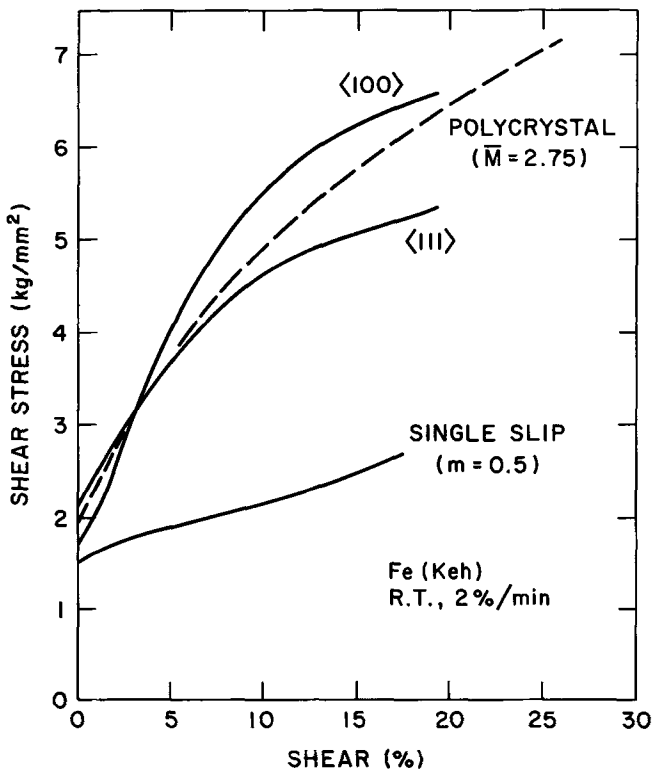


Fig. 17—Shear stress vs shear curves for 99.95 pct Fe (Ferrovac E): three single crystals of controlled orientations and one polycrystal of a grain size of 0.1 mm (15 pct surface grains). After Keh.<sup>73</sup>

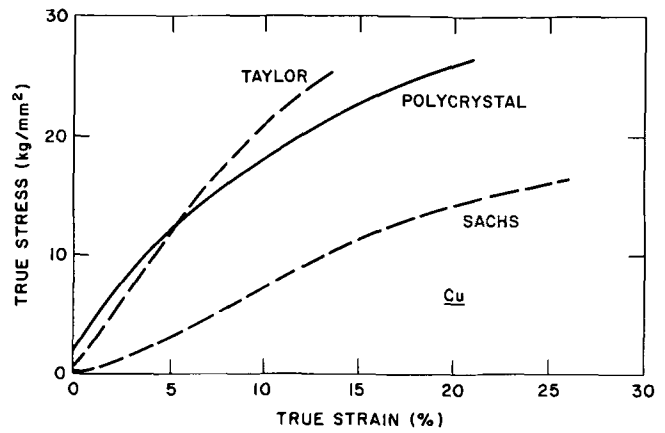


Fig. 18—Tensile stress-strain curve for a polycrystal of 99.98 pct Cu, grain size 0.15 mm (10 pct surface grains), at room temperature. Dashed lines represent theoretical polycrystal curves, derived on the basis of the Sachs model from an average single-crystal curve and on the basis of the Taylor model from a single crystal of an orientation near  $\langle 111 \rangle$ . After Kochendörfer and Swanson.<sup>64</sup>

aluminum polycrystal curve more closely resembles in character that of the  $\langle 111 \rangle$  single crystal in which 6 systems are in fact observed to operate. Some experiments<sup>10</sup> have, in fact, shown exact agreement between polycrystal and  $\langle 111 \rangle$  single crystal in aluminum,\* but more commonly the polycrystal curve is

\*It is possible that some  $\langle 111 \rangle$  texture remained in the drawn polycrystal wires after annealing although it was not visible in Laue back-reflection photographs.

observed to be somewhat lower in level. An explanation of this effect will have to await a more quantitative understanding of stage III in general.<sup>72</sup>

The fact that the polycrystal curve falls within the range of those of single crystals is in itself noteworthy. As a counter example, the tensile stress strain curve for polycrystals of magnesium, which does not have enough independent slip modes to make the Taylor theory applicable, lies far above all free single-crystal tensile curves.<sup>74</sup>

There is certainly room for some modifications of the theory (Eqs. [27]), for example along the lines suggested in Eqs. [28] and [29], without leading to any serious disagreement with the experiments on fcc and bcc materials. However, a major change in the model, for example to the one based on single slip on the most favored system (Eqs. [32]), in addition to being theoretically unsatisfactory, is precluded by the experiments.

This is illustrated in Fig. 18 where the tensile stress strain curve for a copper polycrystal is compared<sup>64</sup> to the tensile curves predicted from the single crystal shear curves\* according to the rival models.

\*Taken from Diehl's<sup>75</sup> work on the identical material.

For the Taylor model, the  $\langle 111 \rangle$  curve was used as a basis for the prediction, for the Sachs model an "average" single crystal curve was used,<sup>64</sup> which is characteristic of single slip and consistent with the basis of the model.

At first sight, neither one of the predictions appears very satisfactory. However, the " $\langle 111 \rangle$  curve" used for the Taylor model was in fact taken from an orientation about 10 deg away from the  $\langle 111 \rangle$  orientation.



The single crystal curves are very sensitive to orientation in this range; specifically,<sup>10</sup> there would be no trace of easy glide in a true  $\langle 111 \rangle$  curve, and the yield stress would be about equal to the stress at the beginning of stage II in single slip curves. Thus, the plotted "Taylor" curve should be shifted to the left by a few percent.<sup>10</sup> The agreement with the polycrystal curve would then be satisfactory near the yield stress and in the rapid hardening region, whereas it would be mediocre in stage III—much like in the cases of aluminum and iron. The discrepancy could be avoided by taking a proper average between the curves of the different polyslip types.<sup>12</sup>

The prediction according to Sachs could be modified, according to Kochendörfer,<sup>41</sup> by the addition of an adjustable but constant stress (Eq. [32a]). Fig. 18 shows that this procedure could lead to agreement in stage III, but would then imply very poor agreement at the yield stress and in stage II. This is a disagreement in kind, not just in degree, and could not have been avoided by using any other "average single slip curve".

#### Temperature and Strain Rate Dependence

More important than any quantitative agreement between a set of stress strain curves under special conditions, from the point of view of showing a close relation between single-crystal and polycrystal plasticity, would be a similar variation of these curves with other deformation parameters. Fig. 16 already showed single-crystal and polycrystal curves at two strain rates differing by a factor 100; the behavior is obviously similar.

Fig. 19 shows polycrystal curves at the same two strain rates but at a wide range of temperatures.<sup>72</sup> One recognizes the typical behavior known from single-crystal deformation: the curve may be decomposed into an initial steep portion that is temperature and rate insensitive ("stage II"), and a progressively flatter portion that is more strain rate sensitive and

very temperature sensitive ("stage III"). The fact that "stage II" in polycrystals is not generally exactly linear does not invalidate this comparison; one reason for a general rounding off may be found in the spread of shear strains in the various grains as discussed in the last section.

Knöll and Macherauch<sup>76</sup> published a similar set of curves for copper polycrystals between 90° and 295°K. In this temperature range, stage III in copper is relatively steep but not very temperature sensitive. This fact, together with the somewhat rounded appearance of stage II, make a determination of the average stage II slope and of the stress at the beginning of stage III difficult. The values given by Knöll and Macherauch show a larger temperature dependence of the stage II slope and a smaller temperature dependence of the stress at the onset of stage III than the corresponding values quoted for single crystals; both deviations are in the right direction to be explained away by the above argument.

In single crystals, one carefully distinguishes between the rate and temperature sensitivity of the *continuous* stress strain curves, as in Figs. 16 and 19, and that of the flow stress at a given history ("strain rate cycling", "temperature cycling"). Fig. 20 shows the rate sensitivity of the flow stress as a function of the flow stress obtained in previous deformation, for single crystals of various orientations and for polycrystals of aluminum.<sup>72</sup> The polycrystal behavior is again similar to that of single crystals and especially close to that of the  $\langle 111 \rangle$  orientation.

In fact, the strain rate sensitivity of single crystals is much less orientation dependent than the stress strain curves themselves, but it clearly differentiates between stage II and stage III.<sup>72</sup> The agreement shown between the polycrystal and the single crystals throughout stages II and III is thus a significant indication of the comparability of the deformation mechanisms in both and makes the lack of a quantitative agreement

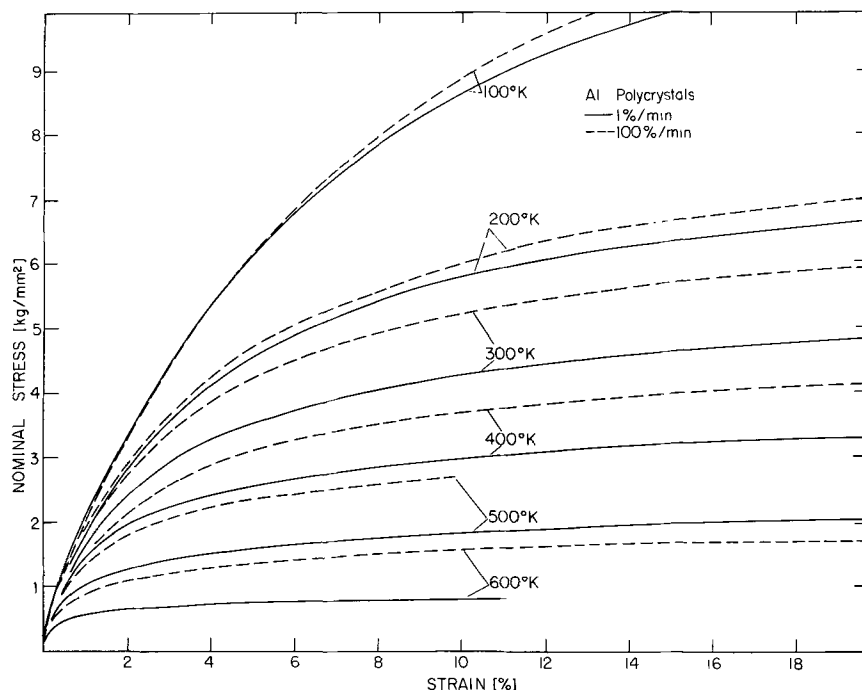


Fig. 19—Tensile stress-strain curves, at two tensile strain rates and at various temperatures, of 99.99 pct Al polycrystals of a grain size of 0.2 mm (15 pct of the grains being on the surface). After Kocks *et al.*<sup>72</sup>

on the stage III stress strain curves themselves seem even less important.

At high temperatures, the discrepancy between the results from strain rate cycling and from the continuous stress strain curves becomes more striking.<sup>72</sup> Fig. 21 shows the rate sensitivity of aluminum polycrystals and  $\langle 111 \rangle$  single crystals at 600°K: they are very similar. Fig. 22, on the other hand, shows that the stress strain curves, again converted to shear by the Taylor formula, are quite different: the polycrys-

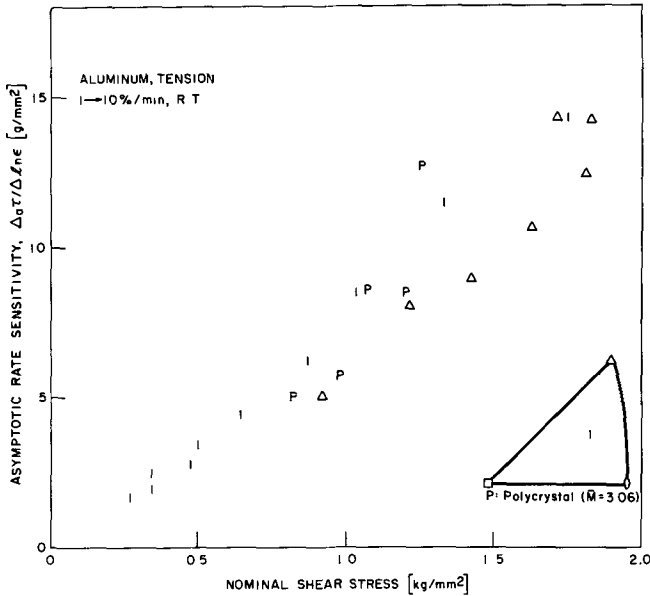


Fig. 20—Rate sensitivity of the back-extrapolated flow stress of aluminum single and polycrystals at room temperature, as a function of the flow stress reached in pre-straining. After Kocks *et al.*<sup>72</sup>

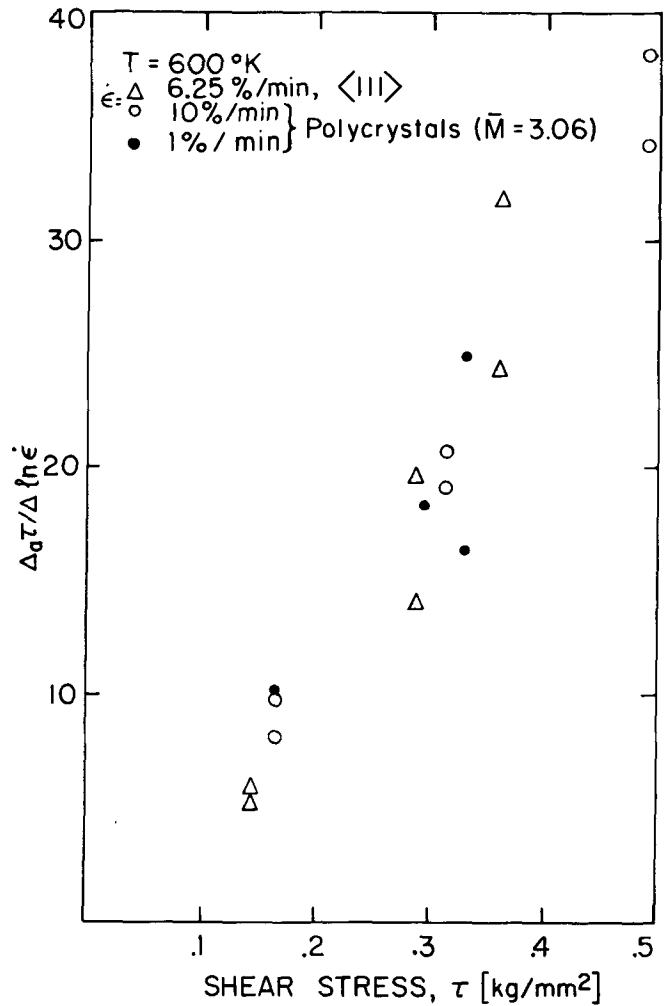


Fig. 21—As Fig. 20, but at 600°K.

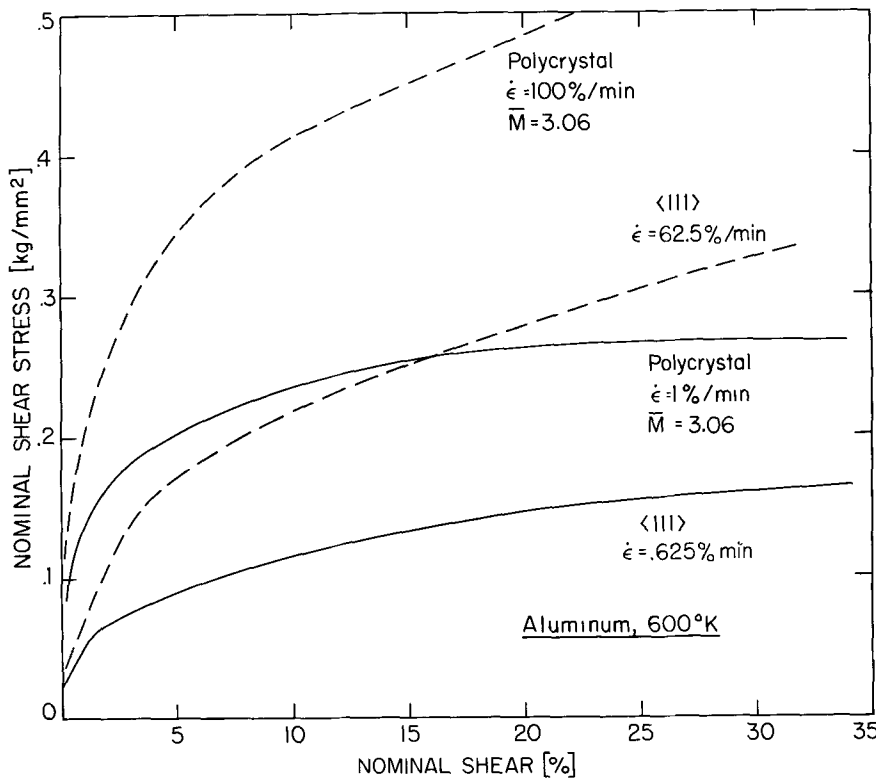


Fig. 22—Shear stress vs shear curves (without correction for area or orientation changes), at two strain rates, for a polycrystal and a single crystal of  $\langle 111 \rangle$  orientation of 99.99 pct pure Al at 600°K. After Kocks *et al.*<sup>72</sup>

tal curve appears displaced upward in the manner proposed by Kochendörfer<sup>41</sup> (Eq. [32a]). Howe and Elbaum<sup>77</sup> suggest that this might be due to an additional contribution from dislocation pile-ups at grain boundaries, since the dislocation mean free path has, at these temperatures, become larger than the grain diameter. Nevertheless, stage III behavior seems to govern the strain dependence and the strain rate dependence of the flow stress.

Temperature cycling experiments were undertaken on copper polycrystals<sup>78</sup> and single crystals<sup>78a</sup> by Bullen and coworkers. Their results show only minor differences between the two.

In summary, the Taylor theory of polycrystal deformation gives quantitative agreement, to within the accuracy of the experiments, with many observations in fcc and bcc materials. Where quantitative agreement is lacking, namely with respect to the flow stress at high strains, it is lacking because of an inadequate understanding of stage III in single crystals, and agreement is by no means excluded by present experiments.

The stages II and III of work hardening in single crystals are found in their major characteristics also in polycrystals.<sup>79</sup> Easy glide is absent in polycrystals. The elasto-plastic transition region, which has sometimes been referred to as "stage 0" in single crystals, has unfortunately been labeled "stage 1" in polycrystals by Schwink;<sup>65</sup> not surprisingly, it was found to have no relation to easy glide, the stage I of single-crystal work hardening.<sup>66</sup>

#### GRAIN BOUNDARY EFFECTS

All the effects of interactions between grains discussed up to now would be present also if the deformation within each grain were homogeneous and uniform. The fact that, for various reasons, it is not, may bring in effects depending on the grain size.

Some nonuniformities in the deformation are due to the boundary conditions in each grain. Firstly, as we have seen in the foregoing, the necessity to maintain equilibrium across grain boundaries, when the stress state in each grain is discrete, requires an internal stress field with a characteristic wavelength of the grain diameter. Although the response to this stress field was assumed to be elastic in the Eshelby-Kröner model, there may well be some plastic relaxation near the grain boundaries.

Secondly, the individual grains adjacent to any particular grain do have characteristics of their own, which make the boundary conditions vary along the periphery of the particular grain considered. This influence may fragment the grain into domains of more nearly uniform deformation. Note, however, that the Taylor theory is applicable to volume elements of any size, not only to entire grains: the compatibility conditions have to be obeyed everywhere.\*

\*M. F. Ashby (private communication) has recently considered the possibility that the dislocations stored to accommodate these incompatibilities due to non-uniformity contribute directly to the yield strength. He finds that this would lead to a proportionality between the yield strength and the square root of a quantity that consists of a sum of a constant and the inverse grain size.

Finally, nonuniformities in deformation are due to the inherent heterogeneity of slip and dislocation movement.

The fact that slip is restricted to planes about 1  $\mu\text{m}$  apart, which develop substantial slip steps on free surfaces, but cannot do so on grain boundaries, may in principle cause additional strengthening in a polycrystal. These effects have been named "microscopic compatibility conditions" by the Chalmers group who did critical experiments to investigate their importance.<sup>80-83,6</sup>

In bicrystals under any general state of stress, the macroscopic compatibility conditions<sup>84</sup> demand the operation of a total of four slip systems in both crystals,<sup>81,83,16</sup> whereas the individual crystals would slip on only one system each, if they were free. The forced operation of an additional slip system, generally on an intersecting plane, should force an increase in work hardening as was indeed observed. Fig. 23 gives some examples.

The prime effect of the interaction between grains is a tendency to eliminate easy glide. In the case of the  $\langle 210 \rangle$  bicrystal, the effect persists to larger strains.  $\langle 210 \rangle$  single crystals always deform on a single slip system, although this system may be one or the other of the two equally stressed systems in different regions of the specimen, Fig. 24.<sup>6</sup> In the bicrystal, the two systems are forced to interpenetrate,

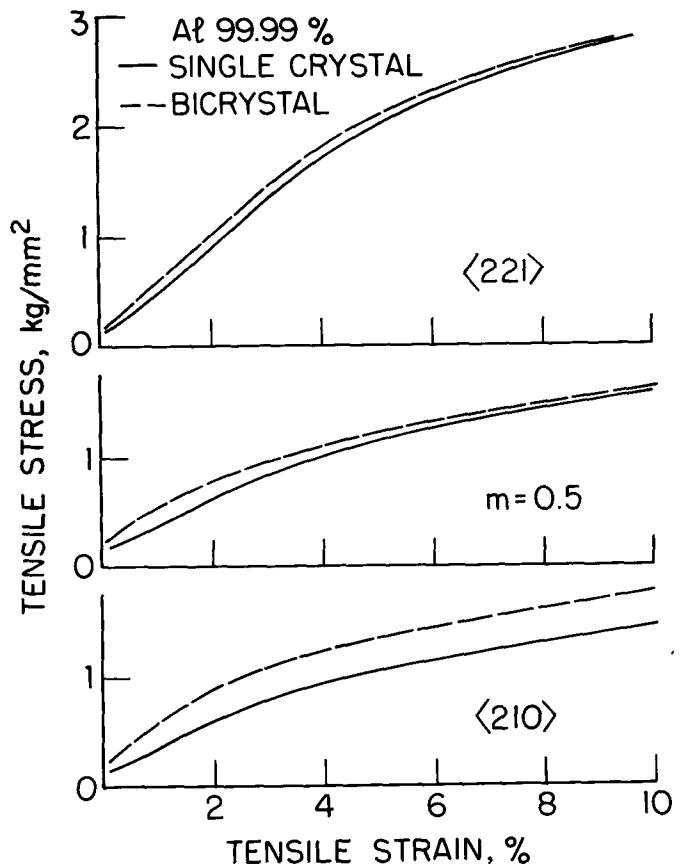


Fig. 23—Single crystals of various orientations and bicrystals which were obtained by rotating one component crystal with respect to the other by 45 deg around the tensile axis. Cross section of each component crystal:  $\frac{1}{4}$  by  $\frac{1}{4}$  in. From Kocks.<sup>6</sup>

causing considerably higher work hardening.\*

\*For the same reason, the  $\langle 100 \rangle$  single crystal is not characteristic of polyslip since, of its eight equally stressed slip systems, two to at most four are observed to operate in any large region in free single crystals.<sup>6</sup>

By contrast, single crystals of  $\langle 211 \rangle$  orientation slip on both the primary and the conjugate slip system everywhere. Since the amounts of slip in the two systems provide two independent parameters,  $\langle 211 \rangle$  bicrystals show the same stress strain curve as single crystals. So do all bicrystals of symmetric orientations in which at least two slip systems are in fact observed to operate in the single crystals.<sup>80</sup> The predominant influence of the macroscopic compatibility conditions is thereby again evident.

There is one other kind of special bicrystal which behaves exactly like single crystals; namely a bicrystal in which the orientation relationship between the two grains is selected such that single slip in each grain would fulfill the macroscopic compatibility conditions at the boundary. No significant effects of any microscopic compatibility conditions were observed.<sup>81</sup>

The stress concentrations ahead of a slip band which meets a grain boundary can be partially relieved by slip on some system in the other grain.<sup>81,83,29</sup> The remaining microscopic incompatibilities would be expected to affect a volume that extends on either side of the grain boundary to a distance comparable to the slip plane spacing. One might thus expect any such effects to be negligible in bicrystals big enough to be tested. In fact, differences observed upon a variation of the specimen size<sup>82</sup> were at the limits of detectability.

In fine-grained polycrystals, on the other hand, one may expect that the volume in which internal stresses cannot be relieved by polyslip may be an appreciable fraction of the specimen. To estimate the order of magnitude of such effects, let us assume that a polycrystal with average grain size parameter \*  $D$  may

\*We do not distinguish between the various parameters such as grain diameter, grain boundary area per unit volume, and so forth. If the truly relevant parameter for a particular case is expressed in terms of a length, the relations derived here hold to within a constant factor.<sup>85</sup>

be regarded as a composite of the material inside the grains, having a flow stress  $\bar{\sigma}$  according to the Taylor model, and a "sponge" of which each "web" is made up of the material near grain boundaries, having a strength  $\sigma_B$  and extending a distance  $d$  (of the order of the slip plane spacing) on either side of the grain boundary. Averaging these two strength contributions over the cross section would give for the composite strength

$$\sigma \approx \bar{\sigma} \left\{ 1 + 4 \frac{d}{D} \left[ \frac{\sigma_B}{\bar{\sigma}} - 1 \right] \right\} \quad [34]$$

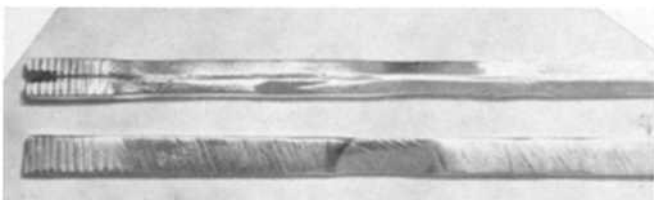


Fig. 24—A single crystal and a bicrystal of aluminum, deformed by tension in a  $\langle 210 \rangle$  direction. The interpenetration of the primary and the critical slip system is more severe in the bicrystal. From Kocks.<sup>6</sup>

In an extreme case, for  $d \approx 1 \mu\text{m}$ ,  $D \approx 10 \mu\text{m}$ , a 50 pct higher grain boundary strength would give a 20 pct rise in flow stress. Such an effect may well show up in fine-grained material. It depends on  $1/D$  and should raise the stress *proportionately* at all strains.

"Notch sensitive" materials, in which a local stress concentration can cause the generation of dislocations or of cracks that spread at lower stresses, are in a different class altogether. Here, microscopic compatibility conditions are of prime importance. Any effect on the flow stress enters as  $1/\sqrt{D}$ , either because of the stress concentration due to a pileup,<sup>86</sup> or because of the process of emission of dislocations from a ledge in a grain boundary.<sup>87</sup> However, as we have seen, the mode of yield is not quasihomogeneous by the polyslip mechanism, but heterogeneous by the propagation of a Lüders band. We have excluded such cases from consideration in this paper; they have been extensively reviewed by Macherauch.<sup>88</sup>

Armstrong *et al.*<sup>89</sup> gave a quantitative treatment of an intermediate case. They conclude that the grain size dependence according to this mechanism should be weaker the smaller the excess of the dislocation generation stress over the propagation stress.

#### Finite Slip Distance. Experiments

We have now considered the effect of slip restricted to discrete planes. Additional effects may be expected because slip in single crystals does not usually progress through even an entire plane; beyond easy glide, dislocations have a mean free path of typically about 100 to  $10 \mu\text{m}$ , inversely proportional to the stress.<sup>90,66,69</sup> One may postulate that the basic mechanism of deformation is undisturbed when the grain diameter is larger than the intrinsic slip distance, but that grain boundaries do limit the dislocation mean free path if they are closer to each other than the slip distance would be in a single crystal under the same conditions. When the grain size is small, one would then expect to start the single-crystal stress strain curve at the stress level corresponding to a slip distance equal to this grain size. From here on the dislocation density should increase as in single crystals and should limit the slip distance in the work-hardened state. The theoretical stress strain curve for polycrystals derived by the Taylor method from single-crystal data should thus be shifted to the left to obtain the polycrystal stress strain curve for smaller grain sizes.

The most extensive investigations of fcc polycrystals after various annealing treatments (and thus various grain sizes) and, in addition, at various strain rates and temperatures were undertaken by Carreker and Hibbard.<sup>91-93</sup> Only in copper<sup>91</sup> did they find a meaningful grain size effect; in aluminum,<sup>93</sup> they detected no effects beyond the scatter of the experiments; silver<sup>92</sup> was, at best, a borderline case in which, unfortunately, the number of grains in the cross section was also too small. In Fig. 19, we have cross-plotted their results for copper at a test temperature of 77°K. The grain size varies by a factor of 8 (and so does, unfortunately, the fraction of surface grains: from 5 to 40 pct). The curves for the smaller grain sizes were shifted to the right until the initial parts of their

stress strain curves coincided. The agreement at high strains is still reasonable.

Conrad and Feuerstein<sup>94</sup> also derived a grain size dependence on the basis of a limited slip distance—but they assumed that grain boundaries form the *only* obstacles to slip. In such a case, one obtains a flow stress that is proportional to  $1/\sqrt{D}$ —but it is also<sup>95</sup> bound to be proportional to the square root of the strain.\* This mechanism may apply to the transition

\*As discussed, the work hardening in stages II and III together may be mistaken for a square-root relation unless the temperature is very low or the range of strains investigated very large.

from the single-crystal yield strength to the raised flow stress corresponding to a mean slip distance equal to the grain diameter, Fig. 25.

From a phenomenological point of view, it may be hard to separate a  $1/\sqrt{D}$  dependence from a  $1/D$  dependence, especially if the latter has an upper cut-off size. This is schematically illustrated in Fig. 26. Published plots of experimental points in a  $\sigma$  vs  $1/\sqrt{D}$  diagram in fact often show a marked curvature<sup>94</sup> such as it would be expected if the real relation were  $\sigma \propto 1/D$ . Additional problems arise from the tendency of many workers to extrapolate their grain size plots to the yield stress of free single crystals.<sup>76</sup> As we have seen, this yield stress is often a property of easy glide, whereas the yield stress of polycrystals ought to relate to the onset of stage II work hardening in single crystals.

#### Grain Boundary Sliding and Grain Boundary Migration

It is often wrongly stated that the Taylor analysis of polycrystal deformation is based on an assumption that grain boundaries do not slide.

The compatibility conditions were stated in the foregoing in terms of the fit between a deformed grain and the deformed "hole" made by its surroundings. It is easy to see that, in the example of an ellipsoidal "hole", rotation of the grain (involving grain boundary sliding) around the rotation axis of the ellipsoid would not change any of the "fit" conditions.

At a small plane element of a grain boundary (assumed perpendicular to the y-direction), the compati-

bility conditions require that  $\epsilon_{xx}$ ,  $\epsilon_{zz}$ , and  $\epsilon_{xz}$  be the same on either side.<sup>84,81</sup> Grain boundary sliding, on the other hand, would contribute a local strain in the  $\epsilon_{yx}$  or  $\epsilon_{yz}$  component; it can thus not relieve any of the compatibility conditions.

Grain boundary sliding may nevertheless occur as a process incidental to slip, as it has in fact been observed.<sup>96</sup> It can provide an *independent* component of the macroscopic strain only if whole sheets of grains extending over the entire cross section slide over each other. Mixed grain boundary sliding and concentrated slip or kinking are a variation of this local mode of yield.<sup>3\*</sup>

\*Grain boundary sliding may affect slip indirectly by providing dislocation sources at ledges in the boundary. This process may be rate controlling at grain sizes so small that dislocation sources are scarce. This process can lead to "superplasticity" (T H Alden, *priv comm.*)

A situation similar to that of grain boundary sliding exists with respect to grain boundary migration. Small angle grain boundaries have been observed to migrate (*i.e.*, move in the direction of their normal) under stress;<sup>97</sup> whether large angle boundaries do is an open question. In any case, the strain contributed locally by grain boundary migration would occur in precisely the same components as grain boundary sliding, *i.e.*,  $\epsilon_{yx}$  or  $\epsilon_{yz}$ ; it cannot relieve any of the strains required by the compatibility conditions.

The possibility of mass transport through diffusive processes ("Nabarro-Herring creep") may of course relieve the compatibility conditions. The sinks and sources for the moving atoms would have to be at grain boundaries. Inasmuch as it would not matter which *side* of a particular grain boundary element an arriving atom attached itself to, grain boundary migration may be an effect incidental to this process.

#### SUMMARY

The following results, reported by the author at various times, are published here for the first time.

##### Yield Surfaces

1) Description of all strains and rotations due to all slip systems in fcc crystals in terms of crystallographic cubic axes.

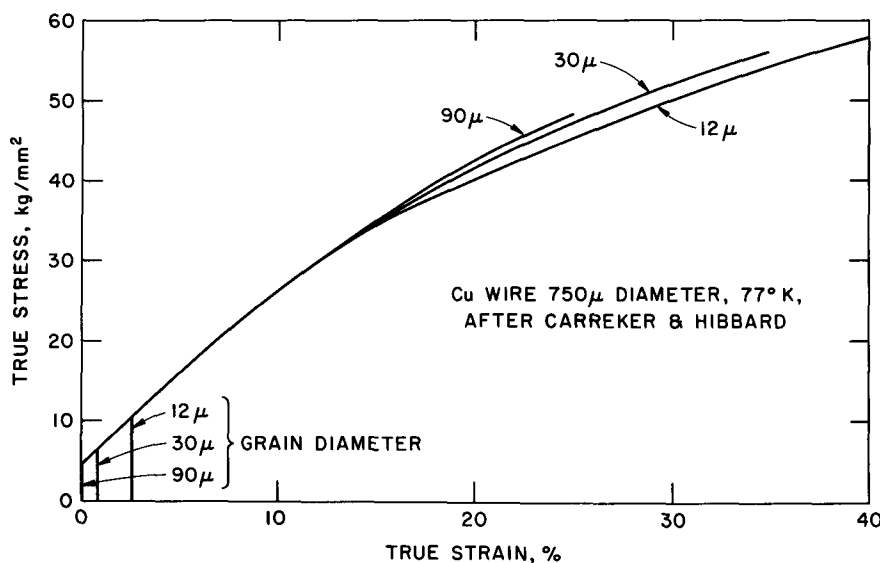


Fig. 25—Tensile stress-strain curves for 99.999 pct Cu polycrystals of various grain sizes.<sup>91</sup> The original curves have been shifted along the horizontal axis to bring their initial portions into coincidence: in the smaller grains, the dislocation mean free path is limited from the start to a value characteristic of some degree of work hardening.

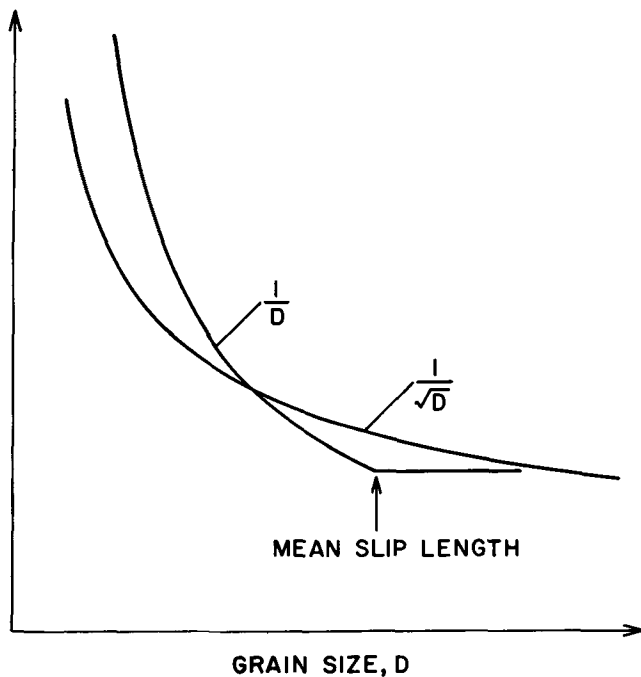


Fig. 26—Comparison of an inverse square root grain size dependence to a dependence on the inverse first power below a certain critical size.

2) Sections through the fcc yield surface (rather than projections as Bishop<sup>7</sup>) and enumeration of the slip system combinations in all corner states.

3) Derivation of the possible axes of arbitrary rotations in polyslip for fcc crystals.

4) Derivation of the identity of the yield surfaces for  $\{111\}\langle 1\bar{1}0\rangle$  slip in fcc crystals and  $\{1\bar{1}0\}\langle 111\rangle$  slip in bcc crystals.

5) Explanation of the similarity of the deformation textures in bcc materials in tension and fcc materials in compression, and vice versa.

6) Prescription for obtaining card glide and pencil glide yield surfaces from the respective yield locus for crystallographic slip.

7) Derivation of lower and upper limits for the average Taylor factor in bcc crystals, independent of slip mode: 2.65 and 3.06.

8) Statement of the most general condition under which pencil glide provides five independent slip modes: the existence of three noncoplanar, *nonorthogonal* slip directions.

### Polycrystals

9) Description of the stress path on the single-crystal yield surface of a grain in an elasto-plastic polycrystal.

10) Prediction of a preponderance of  $\{211\}$  slip in polycrystals of bcc metals in which there is no crystallographic preference for a slip plane in the single crystals.

11) Derivation of the equivalence of Taylor's minimum shear sum hypothesis and the yield condition.

12) Discussion of the assumptions inherent in converting polycrystal stress strain curves into shear stress shear sum curves by the Taylor method.

13) Report of some bicrystal experiments showing the importance of latent hardening.

14) Report of some observations of latent hardening in polyslip.

15) Discussion of effects depending on the inverse of the grain size and on the mean slip distance in single crystals; reevaluation of some relevant experiments in the literature.

16) Derivation of the irrelevance of grain boundary sliding and grain boundary migration.

*Reviewing* the field of homogeneous plasticity (as opposed to deformation by the spreading of a Lüders band) in polycrystals at sub-diffusive temperatures, we come to the following conclusions.

The relation between polycrystal and single-crystal flow stress and work hardening, including their dependence on temperature and strain rate, is well established for fcc and bcc materials. The conversion of polycrystal stress strain curves into shear stress shear sum curves by the Taylor method, and its comparison to single-crystal data in polyslip, is quantitatively correct to the degree of accuracy to be expected. In stage III, a better understanding of single crystal behavior is necessary.

The derivation of the deformation textures in bcc materials should now be straight-forward; in fcc materials it has yet to be determined which of various effects determines the otherwise arbitrary components of rotation in many grains.

Genuine grain size effects, in the absence of a yield drop and of diffusive mechanisms, are negligible except at very small grain sizes where they should be proportional to  $1/D$  rather than  $1/\sqrt{D}$ , in many cases.

### ACKNOWLEDGMENTS

Lively discussions throughout many years and detailed comments on the manuscript by Drs. A. S. Argon, M. F. Ashby, G. Y. Chin, and W. F. Hosford, Jr., are gratefully acknowledged.

A considerable portion of the work reported in this paper was done between 1955 and 1965 while the author was affiliated with the Division of Engineering and Applied Physics, Harvard University, Cambridge, Mass., and was there supported by the Office of Naval Research under contract Nonr 1866(27). The balance of the work was performed at Argonne National Laboratory under the auspices of the U.S. Atomic Energy Commission.

### REFERENCES

1. L. A. Johnson, U. F. Kocks, and B. Chalmers: *Scripta Met.*, 1968, vol. 2, pp. 265-70.
- 1a. L. A. Johnson: *Trans. TMS-AIME*, 1969, vol. 245, pp. 275-82.
2. E. Schmid: *Proc. Int'l. Cong. Appl. Mech.* (Delft), 1924, p. 342.
3. F. A. McClintock and A. S. Argon: *Mechanical Behavior of Materials*, Addison-Wesley, 1966.
4. G. Y. Chin, R. N. Thurston, and E. A. Nesbitt: *Trans. TMS-AIME*, 1966, vol. 236, p. 69.
5. T. H. Lin: *J. Franklin Inst.*, 1960, vol. 270, pp. 291-300.
6. U. F. Kocks: Ph.D. thesis, 1959, Harvard Univ., Cambridge, Mass.
7. J. F. W. Bishop: *Phil. Mag.*, 1953, vol. 44, pp. 51-64.
8. A. V. Hershey: *J. Appl. Mech.*, 1954, vol. 21, pp. 241-49.
9. U. F. Kocks and T. J. Brown: *Acta Met.*, 1966, vol. 14, pp. 87-98.
10. U. F. Kocks: *Acta Met.*, 1958, vol. 6, pp. 85-94.
11. W. F. Hosford, Jr.: *Trans. TMS-AIME*, 1965, vol. 233, pp. 329-33.
- 11a. G. Y. Chin, E. A. Nesbitt, and A. J. Williams: *Acta Met.*, 1966, vol. 14, pp. 467-76.
- 11b. E. W. Kelley and W. F. Hosford, Jr.: *Trans. TMS-AIME*, 1968, vol. 242, pp. 5-13, 654-60.
12. U. F. Kocks: *Acta Met.*, 1960, vol. 8, pp. 345-52.

13. G. I. Taylor: *J Inst Met*, 1938, vol. 62, pp. 307-24; *S Timoshenko Anniversary Volume*, pp 218-24, Macmillan, 1938; *Deformation and Flow of Solids*, pp. 3-12, Springer, 1956.
14. G. Y. Chun, W. L. Mammel, and M. T. Dolan *Trans TMS-AIME*, 1967, vol. 239, pp. 1854-55.
15. W. F. Hosford, Jr.: *Acta Met*, 1966, vol. 14, pp. 1085-94.
16. U. F. Kocks: *Phil Mag.*, 1964, vol. 10, pp. 187-93
17. H. R. Piehler *Met. Trans*, 1970, vol. 1, in press.
18. W. F. Hosford, Jr., private communication, Univ. of Michigan, Ann Arbor, Mich.
19. U. F. Kocks: *Trans. TMS-AIME*, 1964, vol. 230, pp. 1160-67.
20. B. Ramaswami, U. F. Kocks, and B. Chalmers *Trans TMS-AIME*, 1965, vol. 233, pp. 927-31.
21. O. Knrsement, G. F. deVries, and F. Bell: *phys. stat. sol.*, 1964, vol. 6, pp. 73-81.
22. Y. Nakada and A. S. Keh: *Acta Met.*, 1966, vol. 14, p. 961.
23. P. J. Jackson and Z. S. Basinski: *Can. J Phys.*, 1967, vol. 45, pp. 707-35.
24. E. J. H. Wessels and P. J. Jackson: *Acta Met.*, 1969, vol. 17, pp. 241-48.
25. U. F. Kocks and D. G. Westlake: *Trans. TMS-AIME*, 1967, vol. 239, pp. 1107-09.
26. E. Kroner *Z Physik.*, 1958, vol. 151, pp. 504-18.
27. E. Kroner *Acta Met*, 1961, vol. 9, pp. 155-61
28. J. D. Eshelby: *Proc Roy Soc.*, 1957, vol. A241, p. 376
29. R. E. Hook and J. P. Hirth: *Acta Met*, 1967, vol. 15, pp. 535-51, 1099-1110.
30. J. R. Willis: *Quart. J. Mech. Appl. Math.*, 1964, vol. 17, p. 157.
31. R. Hill: *J. Mech. Phys. Sol.*, 1965, vol. 13, pp. 89-101.
32. H. Payne, S. J. Czyzak, J. H. Greiner, and T. H. Lin: *J. Mech. Phys Sol*, 1958, vol. 6, pp. 314-20.
33. B. Budiansky and T. T. Wu: *Proc. 4th Cong. Appl. Mech.*, 1962, p. 1175
34. J. W. Hutchinson: *J. Mech Phys. Sol.*, 1964, vol. 12, pp. 11-24.
35. W. Voigt: *Wied. Ann.*, 1889, vol. 38, p. 573.
36. A. Reuss: *Z Angew Math. Mech.*, 1929, vol. 9, p. 49.
37. R. Hill: *Proc. Phys. Soc. London*, 1952, vol. A65, p. 351.
38. D. C. Drucker, H. J. Greenberg, and W. Prager: *J. Appl Mech*, 1951, vol. 18, pp. 371-78
39. R. Hill: *Phil Mag.*, 1951, vol. 42, pp. 868-75
40. R. von Mises: *Z. Angew. Math. Mech*, 1928, vol. 8, pp. 161-85.
41. A. Kochendorfer: *Plastische Eigenschaften*, 1941, Springer.
- 41a. G. Y. Chun and W. L. Mammel: *Trans. TMS-AIME*, 1969, vol. 245, p. 1211
42. J. F. W. Bishop and R. Hill *Phil Mag.*, 1951, vol. 42, pp. 414-27, 1298-1307.
43. R. Hill: *J. Mech. Phys. Sol*, 1967, vol. 15, pp. 79-95.
44. F. R. N. Nabarro, Z. S. Basinski, and D. B. Holt: *Adv. Phys*, 1964, vol. 13, p. 193
45. H. Tresca: *Mem. Sav. Acad. Sci. Paris*, 1872, vol. 20, p. 281.
46. R. von Mises: *Göttinger Nachr., Math-Phys.*, 1913, p. 582.
47. U. Dehlinger: *Z. Metallk.*, 1943, vol. 35, p. 182.
48. U. Dehlinger, J. Diehl, and J. Meissner: *Z. Naturf.*, 1956, vol. 11a, pp. 37-41.
49. G. I. Taylor: *Proc. Roy. Soc.*, 1934, vol. A145, p. 1.
50. M. Roš and A. Eichinger: *Proc. 2nd Int'l. Cong. Appl. Mech.*, Zurich, 1926, p. 315; see also J. L. M. Morrison *Proc. Inst. Mech. Eng.*, 1942, vol. 144, p. 33.
51. R. Hill: *Math. Theory of Plasticity*, Clarendon Press, Oxford, 1950.
52. W. Sautter, A. Kochendorfer, and U. Dehlinger: *Z. Metallk.*, 1953, vol. 44, pp. 442-553
53. V. S. Lensky: in *Plasticity*, 2nd Symp. Nav. Struct. Mech., Brown Univ., E. H. Lee, ed., Pergamon Press, 1960.
54. G. I. Taylor: in *Deformation and Flow of Solids*, pp. 3-12, IUTAM Colloq. Madrid, 1955, Springer, 1956
55. J. W. Hutchinson: *J. Mech. Phys. Sol.*, 1964, vol. 12, pp. 25-33
56. G. Y. Chun and W. L. Mammel: *Trans TMS-AIME*, 1967, vol. 239, pp. 1400-05.
57. U. F. Kocks: *Can. J Phys*, 1967, vol. 45, p. 1134.
58. J. F. W. Bishop: *J. Mech Phys Sol.*, 1954, vol. 3, pp. 130-42
59. T. H. Lin and B. Lieb: *J. Mech. Phys Sol*, 1962, vol. 10, pp. 65-72
60. See I. L. Dillamore and W. T. Roberts: *Met Rev*, 1965, vol. 10, pp. 271-380.
61. G. Y. Chun. in *Textures in Research and Practice*, J. Grewen and G. Wassermann, eds., pp. 51-80, Springer, 1969
62. G. Sachs: *Z. Verein Deut. Ing.*, 1928, vol. 72, p. 734.
63. H. L. Cox and D. G. Sopwith: *Proc Phys Soc London*, 1937, vol. 49, p. 134
64. A. Kochendorfer and M. Swanson *Arch Eisenhuttentw*, 1960, vol. 31, pp. 549-53
65. Ch. Schwink *phys. stat. sol.*, 1965, vol. 8, pp. 457-74
66. Ch. Schwink and W. Vorbrugg: *Z Naturforsch.*, 1967, vol. 22a, pp. 626-42.
67. U. F. Kocks: *Diplom Thesis*, Univ. of Gottingen, 1954.
68. G. Masang *Lehrbuch der Allgemeinen Metallkunde*, p. 388, Springer, 1950.
69. G. Zankl: *Z. Naturforsch*, 1963, vol. 18a, p. 795.
70. H. Wildorf and D. Kuhlmann-Wildorf: *Z. Angew Physik*, 1952, vol. 4, p. 409
71. U. Essmann, M. Rapp, and M. Wilkens *Acta Met.*, 1968, vol. 16, pp. 1275-87.
72. U. F. Kocks, H. S. Chen, D. A. Rigney, and R. J. Schaefer in *Work Hardening*, pp. 151-75, Gordon and Breach, 1968.
73. A. S. Keh: *Phil. Mag.*, 1965, vol. 12, p. 9.
74. E. Schmid and W. Boas *Plasticity of Crystals*, p. Hughes, London, (original published in 1935).
75. J. Diehl: *Z. Metallk.*, 1956, vol. 47, pp. 331-43
76. H. Knoll and E. Macherauch *Z Metallk.*, 1964, vol. 55, pp. 638-45.
77. S. Howe and C. Elbaum *Phil Mag.*, 1961, vol. 6, pp. 37-48.
78. F. P. Bullen and C. B. Rogers: *Phil. Mag.*, 1964, vol. 9, pp. 401-12.
- 78a. F. P. Bullen and S. McK. Cousland: *phys. stat. sol.*, 1968, vol. 27, pp. 501-12
79. P. Derner and E. Kappler: *Z. Naturforsch*, 1959, vol. 14a, pp. 1080-81, 1082.
80. R. S. Davis, R. L. Fleischer, J. D. Livingston, and B. Chalmers: *Trans AIME*, 1957, vol. 209, pp. 136-40.
81. J. D. Livingston and B. Chalmers: *Acta Met*, 1957, vol. 5, pp. 322-27.
82. R. L. Fleischer and B. Chalmers: *Trans Met. Soc. AIME*, 1958, vol. 212, pp. 265-74.
83. J. J. Hauser and B. Chalmers: *Acta Met.*, 1961, vol. 9, pp. 802-18.
84. D. A. G. Bruggeman: *Doctoral Dissertation*, Utrecht, 1930.
85. F. Rhines: *Met Trans*, 1970, vol. 1, pp. 1105-20.
86. F. R. N. Nabarro: in *Some Recent Developments in Rheology*, p. 38, London, The British Rheologists' Club, 1950.
87. J. C. M. Li: *Trans. Met. Soc. AIME*, 1963, vol. 227, p. 239.
88. E. Macherauch: *Z. Metallk.*, 1964, vol. 55, pp. 60-82
89. R. Armstrong, I. Codd, R. M. Douthwaite, and N. J. Petch. *Phil. Mag.*, 1962, vol. 7, pp. 45-58. (See also this issue.)
90. S. Mader: *Z. Phys*, 1957, vol. 149, p. 73.
91. R. P. Carreker and W. R. Hibbard: *Acta Met.*, 1953, vol. 1, pp. 654-63.
92. R. P. Carreker and W. R. Hibbard: *Trans. AIME*, 1957, vol. 209, p. 112.
93. R. P. Carreker and W. R. Hibbard: *Trans. AIME*, 1957, vol. 209, p. 1157.
94. H. Conrad, S. Feuerstein, and L. Rice: *Mat. Sci. Eng.*, 1967, vol. 2, pp. 157-68.
95. U. F. Kocks: *Phil. Mag*, 1966, vol. 13, pp. 541-66.
96. D. McLean: *Mechanical Properties of Metals*, pp. 303-07, Wiley, 1962.
97. J. Washburn and E. R. Parker: *Trans AIME*, 1952, vol. 194, p. 1076.